From quadrupedal to bipedal walking 'on the fly': the mechanics of dynamical mode transition in primates

Peter Aerts[1,2], Jana Goyens[1], Gilles Berillon[3,4], Kristiaan D'Août[5], François Druelle[1,3,4]

[1]Laboratory of Functional Morphology, University of Antwerp, Antwerp, Belgium
[2]Department of Movement and Sports Sciences, University of Ghent, Ghent, Belgium
[3]HNHP (UMR 7194), CNRS-MNHN-UPVD, Paris, France
[4]Primatology station of the CNRS (UAR 846), Rousset, France
[5]Institute of Life Course and Medical Sciences, University of Liverpool, Liverpool, UK

Running title: quadrupedal-bipedal transitions in baboons

Key words: terrestrial locomotion, primates, locomotor mechanics, quadrupedal-bipedal transitions, *Papio Anubis*

Summary Statement

Mechanical analysis of the smooth, continuous transition from a quadrupedal to bipedal locomotor mode in baboons reveals a common strategy: crouch the hind parts and sprint them underneath the rising body centre of mass.

ABSTRACT

We investigated how baboons transit from quadrupedal to bipedal walking without any significant interruption in their forward movement (i.e. transition on the fly). Building on basic mechanical principles (momentum only change when external forces/moments act on the body), insights into possible strategies for such a dynamical mode-transition are provided and applied first to the recorded planar kinematics of an example walking sequence (including several continuous quadrupedal-, the transition- and subsequent bipedal steps). Body dynamics are calculated from the kinematics. The strategy used in this worked example boils down to: crouch the hind parts and sprint them underneath the rising body center of mass. Forward accelerations are not in play. Key-characteristics of this transition strategy are extracted: progression speed, hip height, step duration (frequency), foot positioning at touch down with respect to the hip and the $BCoM$ and congruity between the moments of the ground reaction force about the $BCoM$ and the rate of change of the total angular moment. Statistical analyses across the full sample (15 transitions of 10 individuals) confirm this strategy always used and shared across individuals. Finally, the costs (in J/kg/m) linked to on the fly transitions are estimated. The costs approximately double those of both the preceding quadrupedal and subsequent bipedal walking. Given the short duration of the transition as such (< 1sec), it is argued that the energetic costs to change walking posture on the fly are negligible when considered in the context of the locomotor repertoire.

INTRODUCTION

Bipedal and quadrupedal locomotion share common biomechanical features in non-human primates and might be controlled by the same basic neuromotor mechanism (for an elaborate discussion on this: see Aerts et al., 2000; D'Août et al., 2004; Druelle et al., 2017a; Higurashi et al., 2019; Nakajima et al., 2004; Nakajima et al., 2001; Zehr et al., 2009). Also, the coordination between fore- (arms) and hindlimbs (legs) in (habitual) bipedal humans is suggested to be the result of the same coupled pattern generators as observed in habitual quadrupeds (Balter and Zehr, 2007; Dietz, 2002; Dietz et al., 2001; Zehr et al., 2009). In this context, it has been hypothesized that the components of the quadrupedal neural circuitry were conserved during the evolution of hominins and used for bipedal locomotion (Zehr et al., 2009). The use of the same neural network would have greatly facilitated the evolutionary transition from quadrupedal animals to bipedal ones. Nevertheless, an evolutionary transition from a quadrupedal ancestor to a habitual bipedal primate likely requires intermediate forms capable of both locomotor modes (Rose, 1991).

Interestingly, all extant Catarrhini species, while largely relying on the quadrupedal locomotor system, are also able of occasional bipedal walking and use this locomotor mode spontaneously in their daily activities (e.g. Druelle and Berillon, 2014; Rosen et al., 2022). The proportion of their bipedal walking has been widely quantified in natural (Carvalho et al., 2012; Hunt, 1994; Rose, 1976; Stanford, 2006; Wrangham, 1980) and experimental contexts (Druelle et al., 2016; Videan and McGrew, 2001; Videan and McGrew, 2002), and also the kinematics of bipedalism in non-human primates have been studied extensively (e.g., Aerts et al., 2000; Berillon et al., 2010; Blickhan et al., 2018, 2021; Demes, 2011; Hirasaki et al., 2004; Nakatsukasa et al., 2006; Ogihara et al., 2010; Thompson et al., 2015; Thompson et al., 2021; for an overview, see Druelle et al., 2022a). Nevertheless, little is known about how primates (or quadrupeds in general) deal with dynamic transitions from quadrupedal to bipedal walking 'on the fly', such as for instance exemplified in figure 1A. Nakajima et al. (2001) mentioned that, at least *Macaca fuscata,* can move from quadrupedal to bipedal walking without any break in their forward speed. Apparently, baboons are also capable of this (Fig. 1A).

The exploitation of such behavioural capacity might have been essential in the evolutionary emergence of habitual bipedalism in hominins. From this point of view, it is important to better understand the mechanics of quadrupedal-bipedal transitions 'on the fly'.

In this context, we investigate the mechanics of 'on the fly' quadrupedal-bipedal transitions in the olive baboon, *Papio anubis.* We chose to focus on this species because it can be considered, among primates, a terrestrially specialised quadruped, frequently showing transitions toward bipedalism in its natural movement repertoire (e.g. Berillon et al., 2010; Druelle et al., 2022b; Rose, 1976). We will first provide a theoretical framework that considers the mechanical options available for a quadruped to perform 'on the fly'-transitions, relating the whole-body level to kinematical and dynamical strategies. Preliminary, qualitative observations of the transitions performed by several specimens of the study population led us to hypothesize that they all, and always, make the transition in a very similar way (i.e. use the same basic strategy). In order to test this, we will first describe in detail, relying on the theoretical framework, the transition mechanics in play for one worked example (containing several quadrupedal steps, the transition and several bipedal steps in sequence) and will then define the kinematical and dynamical key characteristics of the transition. As a last step, we will establish how stereotyped the strategy is across individuals by statistically assessing and discussing the variability of key characteristics. We will thus provide insights in the control strategy used by the baboons to lift the

heavy upper body (head-arms-trunk or HAT; ~75% of body weight) in an orthograde posture during walking. We hypothesize that (1) the transition from quadrupedal to bipedal locomotion is effectively performed 'on the fly', i.e. in a smooth and non-erratic way and without any significant interruption in forward movement. Further, we hypothesize that (2) all individuals use a similar strategy and that, given the spontaneous nature of bipedal behaviours in baboons, (3) the transition can be performed in an efficient way, i.e. implying limited extra costs and efforts compared to the normal quadrupedal and bipedal locomotion. When confirmed, the latter hypothesis supports the above-mentioned point of view on the evolutionary importance of 'on the fly'-transitions in the locomotor repertoire of extinct primates (and potentially in Miocene apes and early hominins).

MATERIALS AND METHODS

Methodological framework Straight forward mechanical considerations provide a way to analyse and interpret the dynamics of 'on the fly' quadrupedal-bipedal transitions of quadruped animals as exemplified in figure 1A. These transitions are characterized by, principally, sagittal plane kinematics and involve considerable reorientation of body segments, mostly represented in the upwards rotation of the heavy Head-Arms-Trunk (HAT) segment (Fig. 1B). This implies considerable changes in the total 'amount of rotational movement' (i.e. angular momentum) of the body (H_{body}; see Fig. 1C). Expressed with respect to the origin of a frame of reference moving with the Body Centre of Mass ($BCoM$; see Fig.1C), the quadrupedal-bipedal transition 'on the fly', can thus be expected to result in a sudden and temporarily rise of H_{body} above its normal oscillations about zero during steady walking.

According to basic mechanical principles, angular momentum can only change as a result of external moments acting on the multi-segmented body. Consequently, in the frame of reference moving with the $BCoM$, the time derivative (instantaneous change) of H_{body} (= $\dot{H}_{body}$; cf. Fig.1C) equals, at any instant, the resultant external moment of the 'total body ground reaction force' (GRF; cf. Fig.1C) about the $BCoM$ [air resistance can safely be neglected (small compared to the $GRFs$), and all moments of the segmental weights (*mg*) and of the segmental fictitious forces as a result of the $BCoM$-accelerations, sum up to zero]. When walking steadily quadrupedally or bipedally, $\dot{H}_{body}$ must fluctuate in a regular way about zero. Hence, the pattern of the moment of GRF about the $BCoM$ is regular, too. However, upon the 'on the fly' quadrupedal-bipedal transition, this regularly fluctuating pattern becomes disrupted. This must be reflected in alterations of the GRF in terms of position and/or orientation and/or magnitude, since the moment of the GRF about the $BCoM$ can only change over time in two (mostly coupled) ways: (i) variation of the magnitude of the GRF and/or (ii) variation of its moment arm (R; see Fig.1C) by either a shift of the point of application (PoA) of the GRF relative to the $BCoM$ and/or by the reorientation of the GRF-vector (Fig.2A-C). However, position, magnitude and orientation of the GRF are the net-representation of all instantaneous (loco-)motor actions by the animal. Therefore, studying the temporary changes of the moment of the GRF about the $BCoM$ and interpreting these in terms of the observed kinematics and dynamics of the body segments can provide insights in the transition dynamics and the underlying control strategies.

'On the fly' transition implies upwards acceleration of the heavy HAT from its initial pronograde posture. $\dot{H}_{body}$ can thus be expected to show (in the reference frame as in Fig. 2A-C) a positive peak. However, towards the end of the transition, the upwards rotating heavy HAT must be *decelerated* again (*i.e.* negative $\dot{H}_{body}$) in order to reach a stable orthograde posture. Consequently, during the transition, the initial counterclockwise moment (in the reference frame as in Fig. 2A-C) of the GRF must rapidly flip over into a clockwise one. This happens when the line of action of the GRF changes from being in front of the $BCoM$ to running behind the $BCoM$, which can be realised by (a combination of) (i) shifting the PoA and (ii) redirecting the line of action of the GRF (more horizontally or vertically; Fig. 2A-C). Both affect the length of the moment arm R, hence also the magnitude of the moment itself. Clearly, these time-fluctuations of the moments of the GRFs (in terms of varying magnitude, orientation and position) are most likely not the control-measures the neuromotor system is directly aiming at. They do reflect, however, the underlying motor-strategy used to carry out the quadrupedal-bipedal transition 'on the fly'.

Let's focus onto the upwards acceleration-phase of the HAT, first. As long as fore- and hind limbs are in contact with the ground simultaneously, the PoA can be moved forward with respect to the $BCoM$

by redistributing the *vertical loads* taken by hands and feet (i.e. more load at the forelimbs). Changes in the horizontal loads by hand or feet do not affect the PoA. Higher relative hand-loading may result from *actively pushing the front parts upwards*, while lower relative loading at the feet can be realised by a downward acceleration of the hind parts (*'dropping the hind parts'*; Fig. 2D). Theoretically, this may happen without affecting magnitude and orientation of the total GRF (i.e. when this redistribution is such that it does not change the acceleration, in magnitude and direction, of the $BCoM$). More likely, however, this total GRF will also change because of the combined limb action and if this goes along with an increase in its propulsive component (forward acceleration) and/or its vertical component (upward acceleration), an additional positive effect on the counterclockwise pitching moment will be the result (larger magnitude and larger R). Notice that, in a quadrupedal posture, lowering the hind parts will automatically cause the trunk to be more erected.

However, inherent to the quadrupedal-bipedal transition, hands lose contact with the ground soon, and keeping the PoA in a more anterior position thus readily requires putting down the feet further forward (*'foot repositioning'*; Fig. 2E). As a result, hind parts may drop to some extend as well, but more important is that (especially early in the single limb stance) hip extensors must contract forcefully to counter the increased moment of the GRF about the hip (Fig. 2E). Such strong hip-extensor activity supports HAT accelerations. Obviously, this will be reflected in the magnitudes and orientations of the GRFs, too.

As mentioned, at the end of the transition, the heavy HAT must decelerate in order to get H_{body} oscillating about zero again during the subsequent steady bipedal walking. It seems very plausible that this deceleration largely results from the gravitational forces acting on the heavy HAT, if needed assisted by subtle reversed actively controlled strategies: reduced forward positioning of the feet (affecting PoA) and stronger hip flexor activity at the end of limb retraction (affecting the GRF at the end of stance). Inevitably, however, this will be reflected in the pattern of the moment of the GRF about the $BCoM$.

From the above it must be obvious that, whether still on all four or already bipedal, creating upward momentum of the HAT can go along with temporarily increased horizontal, forward directed ground reaction forces, hence with temporary forward acceleration of the $BCoM$. This observation is important for two reasons. Firstly, overall whole-body acceleration during forward locomotion as such can purposely be applied as a strategy to make the transition 'on the fly' [compare to a motorcycle going 'wheely' when forcefully accelerating; see Druelle et al., 2022a. Such whole-body acceleration likely explains bipedal running bouts in lizards (Aerts et al., 2003) and probably also in the stiff-bodied cockroaches (Full and Tu, 1991)]. Mechanistically, however, within the locomotor cycles, this will always be reflected in kinematical and dynamical phenomena as previously described. Secondly, (temporary) forward acceleration of the $BCoM$, if present, inevitably implies upward pitching of the body and less grip by the forelimbs on the ground (Aerts et al., 2003; Druelle et al., 2022a). This, together with the fact that forelimbs readily lose ground contact during transition anyway, suggests that the role of the forelimbs in the transition 'on the fly' is probably limited.

Experimental design At the Technical Platform of Motion Analysis of Primates (MAP, Primatology Station of the CNRS, Rousset sur Arc, France; e.g. Anvari et al., 2014; Berillon et al., 2010), we collected data on quadrupedal-bipedal walking transitions performed 'on the fly' by olive baboons, *Papio anubis*. One 'Baumer HXC13' digital camera recorded the sagittal kinematics of the animals at 200 Hz while walking unrestrained on a 6m long walkway (see Fig. 1A). This observational protocol ensures natural,

voluntary and spontaneous behaviour. We also positioned a mirror at the end of the walkway because we observed that it was stimulating their bipedal behaviour, thus allowing us to record quadrupedal-bipedal transitions in the field of view of the camera. Animals approached the mirror and by us tilting the mirror backwards during the approach, baboons (often) made the quadrupedal-bipedal transition proceeding upright on the hindlimbs. Ideally, (single limb) GRFs of the entire transition (quadrupedal steps + transition steps + bipedal steps) should be available. One force plate was built into the walkway hence GRFs could be recorded only occasionally (because animals were walking unrestrained and unconditioned along the track), and logically never for the required series of sequential steps. It will be shown, however, that for the present purpose, GRFs and PoAs can reliably be calculated, making this methodology potentially suitable for video recordings made in the field. Figure 1A shows a representative series of stills taken from our lateral camera. Experiments were approved by the Regional Ethical Committee for animal experimentation of the Midi-Pyrénées Region (Letter MP/01/15/02/08).

The study group consisted of 60 individuals ranging from newborn infants to adults. From the screening of all recorded sequences, 15 could finally be retained for further analysis. Selection criteria were: (1) uninterrupted walking along the walkway including a quadrupedal-bipedal transition, (2) no other animal obscuring the view. These 15 sequences belonged to 10 individuals ranging from 2.85kg to 16.12kg (Table 1).

TABLE 1. Individual information

ID	Name	Mass	Age (year)[1]	Sex	Seq. digitized (n)
V916F	Babar	16.12	4.9	M	1
V936G	Fleur	2.85	0.78	F	3
V902G	Céline	7.62	3.81	F	1
V792BA	Chris	10.33	4.02	M	1
V896BB	Dédé	7.26	2.95	M	4
V792BB	Dictée	6.37	2.23	F	1
V936H	Emeraude	5.45	2.03	F	1
V916J	Filosophie	3.59	1.16	F	1
V908GA	Epine	5.86	2.18	F	1
V936D	Ursuline	14.08	7.62	F	1

[1]If more than one sequence was digitized for an individual, we took the mean age of the individual across all the sequences used in the sample.

Frame by frame, 25 body points were digitized (at 200, 100 or 50 Hz, depending the locomotor speed and cycling frequency of the specimens), defining 15 body segments: head [+ neck; nostrils, back of the head (occiput), eyebrows], trunk [extremity of the tail, base of the tail (sacral vertebrae 3), base of the neck (cervical vertebrae 7)], arm, forearm and hand (left: tip of the 3rd finger, wrist joint and elbow; right: tip of the 3rd finger, metacarpophalangeal joint, wrist joint, elbow, acromion), thigh, shank and foot [left: tip of the 3rd toe, medial malleolus, heel (tuber calcanei), knee joint; right: tip of the 3rd toe,

metatarsophalangeal joint, tarsometatarsal joint, lateral malleolus, heel (tuber calcanei), knee joint, greater trochanter; see Berillon et al. 2010]. As animals could not be marked, the digitisation was more sensitive to noise. Therefore, after the calibration, the raw (position) data were filtered at 7 Hz in Matlab (zero phase shift, fourth order Butterworth; Matlab version R2018b, The MathWorks, Natick, USA).

Linear measures of segmental dimensions were available for all individuals (or for individuals of similar sex and size for Filosophie and Ursuline) used in the present analysis. These data were used as input for geometric modelling (based on Crompton et al., 1996; Druelle et al., 2017b) to obtain for each segment the mass, the relative position of the centre of mass (CoM) along the segment's long axis and with respect to the proximal end, and the moment of inertia about the frontal axis at the level of the segment's CoM (Table A in the supplementary material S1).

It must be noticed that shoulder and hip positions could only be digitized at the camera-side of the animals, meaning that effects of pelvic and pectoral rotations on the planar projection of these markers at the opposite side are not taken into account. Yet, the effects on the position of the contralateral hip and shoulder likely remain small. Girdle rotations up to +/- 15° away from the transversal axis result in deviations in hip and shoulder position of maximally 3.5% of the pelvic and pectoral widths respectively. Still, it is worth mentioning that this may somewhat influence the planar projection lengths, as well as the estimated angular positions, of the thigh and upper arm at the opposite side of the animal, hence also to some extent the position of the CoMs of these elements. In this way, this simplification will affect the calculations as mentioned in the next section. However, given that position errors can safely be expected to be small (cf. above) and given that thigh and upper arm only take together less than 10% of the body mass, the potential errors introduced in this way are assumed to be neglectable in the context of present conceptual planar approach.

Data handling Using these individual morphometrical data and the coordinates of the digitized body points, the position of the $BCoM$ was obtained in each frame as follows:

$$BCoM_{x,y} = {\sum_1^{15} m_i x_i, y_i}/{bm}$$

where $BCoM_{x,y}$ are the x, y coordinates of the $BCoM$, m_i is the mass of segment i and x_i, y_i the coordinates in the sagittal plane of the CoM of segment i , bm the total body mass of the individual. First and second (numerical) time derivatives of the position of the $BCoM$ in the sagittal plane (Euler differentiation) yielded the instantaneous velocities ($B\dot{CoM}$) and accelerations ($B\ddot{CoM}$).

The actual quadrupedal-bipedal transition was determined on the basis of the vertical position and velocity of the $BCoM$. First, the step(s) during which the $BCoM$ shifts upwards were identified. The start of the transition time-interval is set when the vertical $BCoM$-velocity $(B\dot{CoM}_y)$ becomes positive; the end when this velocity drops below zero again (see Fig. 3A).

The average walking speed of the transition bouts (quadrupedal + transitional + bipedal steps) was obtained from the slope of the linear regression of the forward displacement of the $BCoM$ against time (see Fig. 3B). The steadiness of walking throughout the transition was assessed on the basis of the R^2-value of this regression. The closer to 1, the more steady the transition bout is.

Magnitude and orientation of the GRF are given by:

$$GRF_x = B\ddot{CoM}_x \; bm$$

$$GRF_y = (BC\ddot{o}M_y + g)bm$$

Segmental orientation regarding the horizontal axis was calculated for each frame and the first time derivative of these angle provides the angular velocity $\dot{\theta}$ of each segment about its own CoM (see also Fig. 1C). The position of the CoM of each segment with regard to the $BCoM$ can be expressed in polar coordinates (r, ρ; cf. Fig. 1C). The first time derivative of the angular coordinate ($\dot{\rho}$) represents the angular velocity of the segmental CoM about the $BCoM$ (Fig. 1C). These data enable to calculate the total angular momentum of the body (H_{body}) and its instantaneous rate of change ($\dot{H}_{body}$) (for equations see Fig. 1C). Knowing $\dot{H}_{body}$ and the magnitude and orientation of GRF, the point of application (PoA) of GRF (with respect to $BCoM$) can be calculated as:

$$PoA = \frac{\dot{H}_{body} - GRF_x\ BCoM_y}{GRFy}$$

This position can afterwards be recalculated with respect to any other (body)point provided the latter's position regarding the $BCoM$ is known.

We calculated the instantaneous mechanical energy for each segment, as follows:

$$E_i = m_i g y_i + \frac{m(\dot{x}_i^2 + \dot{y}_1^2)}{2} + \frac{I_i \dot{\theta}_i^2}{2}$$

Where m_i is the mass of segment i, g is the gravitational acceleration (9.81 m.s^{-2}), y_i is the instantaneous height of the CoM of segment i, $\dot{x}_i$ *and* $\dot{y}_i$ are the linear velocity of the segment CoM, $\dot{\theta}_i$ is the angular velocity of the segment i in the sagittal plane. The time differential of the energy yielded the instantaneous power fluctuations for each segment.

To obtain maximized estimates for the costs for the transition we assume that no energy-transfer happens between segments and that no elastic recovery occurs. In other words, all mechanical energy input and dissipation come at the expense of muscle activation (notice that actual costs will likely be smaller because of some energy transfer and elastic recovery). For power input (i.e. positive power or energy rate) an efficiency (mechanical power/metabolic power) of .25 is assumed; for negative power (dissipation) the efficiency is -1 (cf. e.g. Alexander, 2003). In this way, instantaneous metabolic power is calculated per segment and then summed over all segments. The time-integral of this total instantaneous power yields an estimate for the metabolic energy-costs for the considered time interval. To determine the transition costs, the coinciding time interval is determined on the basis of $BC\dot{o}M_y$: during the upwards movement this velocity is positive and the zero-crossings of the velocity profile determine start and end of the transition (see above and Fig. 3A). The time integral of the power profile for an identical time-interval just prior to, and immediately following the transition are used as estimate for the according quadrupedal and bipedal walking costs, respectively. It is important to notice that in this way only the metabolic costs to do mechanical work are taken into account. The used efficiency values are assumed to include the costs of force production while doing work. Clearly, isometric force production by muscles also comes with metabolic energy consumption. This is not included in the present estimate. The use of more elaborate cost functions (cf. for instance Alexander, 1997) is beyond the goal and scope of this paper.

Statistical analyses Given the protocol previously described, the data are heterogeneous for what concerns the amount of steps that could be collected before and after the transition. Hence, exact nonparametric *permutation tests* for paired samples are applied to test for differences between 1) the

quadrupedal walking gait and the subsequent transition period as delineated (cf. above), and 2) the transition and the subsequent bipedal walking gait.

Specifically, the variations in the touch down position of the feet relative to the $BCoM$ and hip are tested. Also, the step durations (i.e., the time between consecutive contralateral foot touch-downs) throughout the quadrupedal to bipedal transition are compared. The statistical tests are applied on dimensionless values because the present sample includes individuals of different size. The touch down position of the foot relative to the $BCoM$ and the hip was normalized by dividing its value by the shank length as measured directly on the respective individual (cf. e.g., Aerts et al., 2000; Druelle et al., 2022b). The step duration was made dimensionless by dividing its value by the square root of the ratio of shank length over the gravitational acceleration (see Hof, 1996).

The dimensionless forward velocity and the cost of transport were compared between quadrupedal walking, the subsequent delineated transition and the subsequent bipedal walking. For this purpose, we used quadrupedal and bipedal bouts that were equivalent in length to the duration of the delineated transition. Only when sufficient walking steps were available before and/or after the transition, the comparison could be made. As such, a subsample of 10 'quadrupedal walking to transition'-, and 8 'transition to bipedal walking'-sequences could be retained in these comparisons. By comparing J/kg/m, effects of size and speed are taken into account for the cost of transport.

The contribution of the moment of the vertical and horizontal ground reaction forces to $\dot{H}_{body}$ during the transition is tested using a congruity index, calculated as follows:

$$Congruity\ index_{GRFY} = \frac{\sum_{1}^{n-1}[(M_{GRFY_{n+1}} - M_{GRFY_n})(\dot{H}_{body_{n+1}} - \dot{H}_{body_n}) > 0]}{n-1}$$

with M_{GRFY} the moment of the vertical ground reaction force and *n* is the number of data point in the transition time-interval considered. The contribution moment of the horizontal ground reaction force ($Congruity\ index_{GRFX}$) is calculated in a similar way.

The statistics were conducted using the software for Exact nonparametric inference StatXact 3.1 (Cytel, Inc., Cambridge, MA). The significance level was set at $P<0.05$ for all the tests. The Bonferroni correction lowering the alpha level is applied when multiple comparisons were made between all the components of the transition (i.e., quadrupedal *versus* transition, quadrupedal *versus* bipedal, transition *versus* bipedal); this correction corresponds to 3 trials and is indicated with *P'*. In the following parts, the average values are given with their average absolute deviation (i.e. mean ± average deviation).

RESULTS and DISCUSSION

A) Detailed description of the mechanics of the worked quadrupedal-bipedal transition example

This description is based on a transition bout performed by a juvenile (Fleur, cf. table 1; body mass = 2.85 kg, hip height in bipedal posture ~0.2 m at the day of recording; cf. movie1 of supplementary material S2). This individual and sequence is selected because the field of view and the size of the specimen enabled to analyse 13 sequential steps at once (5 preceding quadrupedal, 2 pure transitional and 6 successive bipedal steps). The result of the entire procedure as described in the Materials and Methods section is represented in *movie1* of the supplementary material S2 (animated stick figure, with the $BCoM$, GRF and PoA added). The orientation and position of the GRF regarding the $BCoM$ being overall consistent with what can be predicted from basic mechanical principles proves the general reliability of the procedure. This becomes especially evident when considering the PoA(relying entirely on the magnitude and orientation of the calculated GRF and on the calculated $BCoM$ position) during the bipedal walking phase: the position of the calculated PoA is always and meaningfully situated within the (fore-aft) boundary of the foot in stance (see supplementary animations (S2-S3)).

Figure 3A illustrates how the transition *sensu stricto* is determined based on the vertical movements of the $BCoM$. Its displacement (blue solid curve) is in amplitude and profile largely similar to that of the $HATCoM$ (blue dashed curve) indicating that the HAT movements (rotation) dominate the transition. Start and end timing of the transition phase (dashed vertical lines) are given by the instants of the according zero-crossings of the vertical velocity of the $BCoM$ (red curve). Pale blue and red regions in this graph (and in all other panels of Fig. 3) accord to the stance phase of the foot (right) at the camera-side and the contralateral (left) foot, respectively. Darker regions are the double stance periods.

Figure 3B represents the forward displacement of the $BCoM$ (black dashed curve) and its linear regression against time (blue curve). Clearly, the transition event itself does not affect the instantaneous walking speed (of 0.45 m/s) and based on the position-time profile alone, the event cannot be detected. This is a real 'on the fly' transition at steady walking speed (R^2 = 0.99; cf. Materials and Methods).

The total angular momentum of the body (H_{body}) and the fraction taken by the HAT (H_{HAT}) throughout the walking sequence are illustrated in figure 3C. Clearly, H_{body} is to a great extend determined by the rotational movements of the HAT (also in the quadrupedal mode; the few bipedal steps are more irregular, which is expected because of the lower stability and the fact the animal comes at a standstill at about time = 4s). The difference between the body and HAT curves is the amount of rotation captured in the hind limb oscillations, which is, overall, (and logically) not very different for quadrupedal-, transition- and bipedal steps. As such, the (changes of) H_{HAT} in the transition phase largely represents the efforts spend in what distinguishes that phase from pure quadrupedal and bipedal walking: the upwards rotation of the HAT. During the quadrupedal walking the H_{body} nicely oscillates about zero as dictated by basic mechanical principles (cf. the Theoretical Framework).

The quadrupedal-bipedal transition seems to be initiated at the instant H_{body} and H_{HAT} reach their maxima during the normal oscillations of quadrupedal striding (first dashed vertical line). Instead of dropping again, the momentum stays high/continues to increase for H_{body} and H_{HAT}, respectively. This happens prior to the next (left) foot placement. Apparently, (a) mechanism(s) other than 'foot repositioning' (cf. the Theoretical Framework), like for instance 'drop of the hind parts' or some

'upwards trust generation' from the arms, are in play early in the transition. However, together with the succeeding left foot touchdown (onset of the red-shaded time-interval, about 13% in the transition phase), H_{body} rises sharply, being suggestive for the importance of 'foot repositioning' for the transition-strategy (cf. Theoretical Framework). During the second half of the same left stance, H_{body} (and H_{HAT}) drop already to zero, and although the $BCoM$ further move upwards during the subsequent step (cf. region spanned by blue double headed arrow in Fig. 3A), the positive H_{body}-peak in this period is nearly entirely captured in the hind limb rotations (red arrow in figure 3C; H_{HAT} remains very small). Apparently, major HAT-reorientations (angular changes) are realized within one single step, and the further upwards movement of the $BCoM$ during the second half of what is defined as the transition-phase (cf. above and Materials and Methods) derives primarily from the upwards vertical displacement of the hip during the second 'transition step' (region spanned by blue double headed arrow in Fig. 3G), not from trunk rotation (cf. Fig. 3D, region spanned by blue double headed arrow).

Whenever the H_{body} curve rises, the derivative ($\dot{H}_{body}$) is > 0, meaning that the GRFs exert a counterclockwise *moment* (even when the momentum itself is still negative). Otherwise, when $\dot{H}_{body}$ < 0 the opposite is true. Figure 3E presents $\dot{H}_{body}$ (blue) together with its components as derived from the horizontal (red) and vertical (green) GRFs. The message from this graph is clear and straight forward: changes of H_{body} (blue peaks) accord (in timing and direction) nearly exclusively with the moments generated by the *vertical* GRFs (green peaks). In other words, fore-aft accelerations seem to play hardly any role of importance in the 'on the fly' quadrupedal-bipedal transition. Moreover, since vertical GRFs always point upwards, the fluctuations about zero of $\dot{H}_{body}$ appears nearly exclusively regulated by shifts of the PoA, not by changes of the magnitude or orientation of the $GRFs$. This is confirmed by plotting the PoA (x 10; green curve) together with $\dot{H}_{body}$ (blue curve; Fig. 3F). Both graphs fluctuate nearly perfectly in phase.

As mentioned in the Theoretical Framework, however, time-fluctuations of the moments of the GRFs (in terms of varying magnitudes, orientations and positions) only reflect the underlying strategy used to carry out the quadrupedal-bipedal transition 'on the fly'. To unravel this, we must therefore now evaluate the potential roles of 'drop of the hind parts', 'arm trust' and 'foot repositioning'.

During approximately the first 13% of what is defined as the transition phase, the diagonal limb pair (right hind-left fore-) is in contact with the ground, with the foot far behind the position of the $BCoM$ (even behind the hip; see Fig. 3H). Therefore, *either* 'drop of the hind parts' *and/or* 'arm push' must be in play during this initial phase of the transition. As argued in the Theoretical Framework, (downwards accelerating) hip-drop and arm-push *can* cause (all or not together) a forward shift of the PoA. Fig. 3G shows that both mechanisms might be in play initially in the transition. The hip (blue curve) is accelerating downwards (region spanned by green double headed arrow), while the vertical distance between fingers and shoulder of the left arm increases (red curve; red arrow indicates end of ground contact). This is further confirmed by the forward displacement of the PoA (in front of the $BCoM$) initially in the transition (red arrow in Fig. 3F), but notice that the observed arm extension can equally well be passive (i.e. no real upwards pushing) because of trunk rotation at the hip.

In the Theoretical Framework, it was also mentioned that lowering the hips as such can cause a re-orientation of the trunk (HAT) *provided* the shoulders keep the same height. However, the (maximal) contribution of such reconfiguration is only a small fraction of the total trunk rotation as shown in figure 3D: based on geometry, at its deepest position, the hip drop can stand for only 16% of the total

rotation. Even during this initial phase (before the left foot touch down), the trunk rotation almost triples what could be expected from the hip drop directly. In other words, it cannot be excluded that arm extension (cf. initial rise of the red curve in Fig. 3G) does contribute to some extent actively to the very initial phase of the quadrupedal-bipedal transition.

For what follows it is important to focus briefly on what causes the oscillation of the hip-height during the transition as illustrated in figure 3G (blue curve between the dashed vertical lines). Figure 3H shows the foot positioning with regard to the hip (and the $BCoM$). The blue curves (full = toe; dashed = heel) represent the position of the right foot regarding the hip (horizontal dashed line at zero position), the red curves represent the left foot. Declining curves correspond to the ground contact phase, rising curves represent the swing phase. The black full line is the position of the $BCoM$ with respect to the hip. It is obvious that the lowering of the hip early in transition is not the result of a pronounced more forward touchdown position of the feet in the transition steps. The more likely explanation for the vertical hip oscillation are the knee kinematics. Knee flexion continues during the stance of the right foot when transition initiates (red arrow in Fig. 3I; full blue curve: right knee angle, dashed blue curve: left knee angle), as well as during the subsequent stance of the left foot (green arrow). As a result, the hip drops during the first part of the transition. The subsequent rising of the hip is, at first glance, somewhat puzzling. There is no obvious limb extension going on during this phase. During the single stance phase of the next right step (coincident with the upwards movement of the hip), the knee angle remains almost constant and the ankle angle decreases (blue arrows in Fig. 3I). However, as a consequence of the 'constant knee angle' in this phase, the hip-knee-ankle configuration forms a quasi-fixed triangle. Since the ankle is in front of the hip, retraction of the limb (i.e. the fixed triangle rotates about the 'ankle-point') must go along with the upwards displacement of the hip. Moreover, this rotation forces the tarso-metatarsal joint into dorsi-flexion which will contribute to the hip-rise, too (as it is illustrated by the small vertical height gain of the ankle in figure 3G; ocher curve, region spanned by double headed arrow). The re-gain in hip height obtained in this way corresponds remarkably well to what can be observed in figure 3G. We will return to the knee behaviour later.

However, at least from the moment the left hand loses ground contact onwards, 'foot repositioning' is the only remaining mechanism that can contribute to the transition, since the hip is at that moment close to its deepest position (and is definitely not accelerating downwards anymore). Despite the fact that the foot positioning at touch down with regard to the hip (i.e. the suspension point of the swinging limb) remains fairly unchanged (Fig. 3H), the foot positioning with respect to the $BCoM$ does change (Fig. 3H): in a sequence of three steps (left-right-left) during the transition, the foot positioning changes from oscillating nearly entirely behind the $BCoM$ in the quadrupedal mode, to oscillating beneath the $BCoM$ in the bipedal mode (Fig. 3H). This can happen because the $BCoM$ moves backwards relative to the hip mainly has the result of the upwards rotation of the heavy HAT, but equally well because the hind limbs become considerably less retracted with regard to the hip during the transition phase (as well as during the subsequent bipedal sequence; Fig. 3H). In other words: smaller steps are made at a higher frequency (remind the overall walking speed is fairly constant; cf. Fig. 3B). This reduced limb retraction actually happens already at the end of the quadrupedal hind limb stance preceding the transition phase (and proceeding during the first 13% of it). This strongly indicates that the reduced limb retraction is definitely part of the transition strategy and is not the consequence of anatomical constraints at the level of the hip. Indeed, early in the transition phase, increase of the hip angle as a result of upwards HAT rotation is still very limited. Moreover, although maximal hip angles at the end

of stance become clearly larger throughout transition, these seem still to be smaller than what occasionally happens during the bipedal walking.

All together and worded in a simplified way, the transition strategy applied in this example sequence could be summarized as: *crouch the hind parts and sprint them underneath the rising* $BCoM$. This does not mean, however, that the transition is made effortless. Figure 3J represents the conservative estimation (no energy transfer between segments, no elastic recoveries) of the metabolic power (cf. Materials and Methods). Integrated over the transition phase and expressed per kg body mass and per unit distance covered, the energy spent in the transition (14.24 J/kg/m) roughly triples that spent during quadrupedal (4.62/J/kg/m) and bipedal (4.67/J/kg/m) walking. Given the magnitudes presented on the graph, it appears that the transition 'on the fly' does not require, however, exceptional efforts. A gentle, playful jump starting from a crouched stand still position of only about 20 cm high, is easy to imagine for the young individual executing the present example sequence. From basic principles (change of kinetic energy during push off equals the work done by all external forces; efficiency of 0.25), the costs for such a gentle playful jump can be estimated to be already about the five-fold of the costs for the transition, while the power requirements exceed those for the transition by even more.

Still, the energy input for the transition must be delivered by muscles working concentrically (positive work). We argue that this must come primarily from the hip extensors. Indeed, figure 3I suggests that early in transition knee extensors work eccentrically (negative work) throughout stance (preventing collapse of the continuously flexing knee). The upwards rotation of the heavy HAT shown in figure 3D must be powered primarily by hip extensors. At the end of the transition the $BCoM$ is still moving further upwards, yet without trunk rotation. The knee is delivering no work (as the knee angle does hardly change). We argued that the vertical translation of the HAT is caused by limb retraction and thus, hip extensor torque must be considered again as the primary motor of this part of the transition phase.

Finally, it is worth mentioning that foot repositioning has important consequences. Although the $BCoM$ moves towards the hip, the latter always stays behind the $BCoM$. This inevitably implies a bent-hip-bent-knee bipedal posture in order to ensure that the support bases of the feet oscillate beneath the $BCoM$ as it is needed for stable bipedal walking. Since bipedal walking in bent-hip-bent-knee walking primates remains hip-driven (cf. above and see Druelle et al., 2022a), but also because body weight and inertial forces during walking tend to collapse the bent hip and knee joints, bipedal walking in non-human primates likely remains a strenuous locomotor mode if kept on long periods (for an elaborate discussion on this: see Druelle et al.,2022a).

B) Testing the hypotheses about the quadrupedal-bipedal transition strategy across the full sample

Hypothesis 1: The transition from quadrupedal to bipedal locomotion is effectively performed 'on the fly'

From Figure 3B it is obvious this holds true for the transition of the worked transition example. The forward velocity is constant over the preceding five quadrupedal steps, the two pure transitional steps and the successive six bipedal steps (linear regression R^2 in figure 3B = 0.99). Although all transitions are executed as a single smooth and continuous movement sequence (see stick figure animations in supplementary material S3; R^2 values of linear regression of the forward displacement throughout the transition always > 0.94), the high constancy of the forward velocity is not entirely confirmed across the full sample. Making use of the dimensionless forward velocity of the hip as the reference for locomotor speed, it appears that the dimensionless forward velocity during the transition phase is statistically indifferent from the dimensionless speed during the preceding quadrupedal phase (*paired permutation test*=-0.89, *P*=0.40; Fig. 4). However, the subsequent bipedal walking happens significantly slower (*paired permutation test*=2.30, *P*=0.008; Fig. 4). Dimensionless locomotor speed as measured from the $BCoM$ does not show a significant result between the quadrupedal phase and the transition, and neither between the transition and the subsequent bipedal walking (*paired permutation test*=1.746, *P*=0.07, and *paired permutation test*=1.65, *P*=0.11, respectively; Fig. 4). During the transition phase, dimensionless $BCoM$ speed is significantly lower than the hip speed (*paired permutation test*=-3.76, *P*=0.0001), because relative to the hip the $BCoM$ moves backwards as a result of the upwards and backwards rotation of the heavy HAT. All in all, across the full sample, baboons slow down a bit when transitioning from quadrupedal to bipedal walking on the fly. Most probably, this slight deceleration is imposed by the experimental setup: the baboons approached the end of the technical platform and were thus forced to slow down and to stop, eventually, their forward movement (cf. Material and Methods). Anyway, an interruption of the forward progression to make the quadrupedal-bipedal transition is never observed (see supplementary material S3). Neither is there a forward acceleration to make the transition possible (cf. Theoretical Framework; see further).

Because of the differences in quadrupedal approaching speed, in cycling frequency and in size of the individuals, the observed duration of the transition phases is variable and ranges from 0.3 to 0.88 seconds, with an average of 0.61 seconds. In practice, it implies that the transition is commonly performed within two steps (11/15), but one transition was performed within three steps and three transitions within one step.

Hypothesis 2: All individuals use a similar strategy

Based on the detailed analysis of the worked example, the strategy of this transition basically boils down to: *crouch the hind parts and sprint them underneath the rising* $BCoM$. Foot positioning shifts from behind to 'in front of' the $BCoM$. Furthermore, the same analysis proves that this 'sprinting' does not imply a sudden and momentary forward acceleration of the $BCoM$, but goes along with an increased frequency of smaller stepping cycles. This strategy appears pretty consistent over the full sample.

- *Crouching the hind parts (at the start of the transition):*

For this, it was tested whether hip height decreases between the initiation of the transition and at 13% of the transition (cf. the description of the worked example). There is a significant decrease in hip height (after size correction, from 1.77±0.18 to 1.73±0.20) between the start of the transition and at 13% of the transition (*paired permutation test*=2.19, *P*=0.02; Fig. 5).

- *Sprint the hind parts underneath the rising $BCoM$ by positioning the feet further forward at higher stepping frequencies:*

The dimensionless step duration (1/step frequency) decreases significantly during the transition, i.e., the amount of time between the last foot touch-down before the transition and the next foot touch-down in the transition decreases significantly (Fig. 6A), but there is no other difference in the interlimb stepping frequency (step 1 *vs* step 2: 3.38±0.52 *vs* 3.51±0.60, *paired permutation test*=-1.29, *P*=0.22; step 2 *vs* step 3: 3.51±0.60 *vs* 3.08±0.85, *paired permutation test*=2.34, *P*=0.01; step 3 *vs* step 4: 3.08±0.85 *vs* 2.67±0.53, *paired permutation test*=1.48, *P*=0.14; step 4 *vs* step 5: 2.67±0.53 *vs* 2.94±0.35, *paired permutation test*=-1.45, *P*=0.19; step 5 *vs* step 6: 2.94±0.35 *vs* 3.28±0.66, *paired permutation test*=-0.74, *P*=0.52).

When considering consecutive *touch-down positions* of the contralateral legs *with respect to the hip,* no significant differences could be found during quadrupedal walking, during the transition and during bipedal walking (1.59±0.18 *vs* 1.70±0.18, *paired permutation test*=-1.56, *P*=0.13; 1.86±0.21 *vs* 1.71±0.24, *paired permutation test*=1.53, *P*=0.13; 1.50±0.26 *vs* 1.52±0.14 *paired permutation test*=-0.16, *P*=0.91, respectively), as well as when the quadrupedal walking is compared to the transition (1.70±0.18 *vs* 1.86±0.21, *paired permutation test*=-1.81, *P*=0.07) and when the transition is compared to the bipedal walking (1.71±0.24 *vs* 1.50±0.26, *paired permutation test*=1.55, *P*=0.09; Fig. 6B.1).

When considering each leg separately (i.e. focussing on consecutive footfalls of the same leg, right and left separately), there is a trend toward a significant difference (very close to the significance threshold), in the touch down position *with respect to the hip* for the leg of which the foot touches down at the onset of the delineated transition (i.e. leg1) when quadrupedal walking and the transition are compared; no differences are found for the other leg (leg2) (Leg1: 1.59±0.18 *vs* 1.86±0.21, *paired permutation test*=-1.963, *P*=0.05; Leg2: 1.70±0.18 *vs* 1.71±0.24, *paired permutation test*=-0.018, *P*=0.98; Fig. 6B.1). This means that the first leg that touches-down at the onset of the transition tends to be positioned more in front of the hip, compared to its position during the previous quadrupedal behaviour.

For what concerns consecutive touch-down positions of the contralateral legs *with respect to the* $BCoM$, no significant differences could be found during quadrupedal walking (0.72±0.20 *vs* 0.78±0.20, *paired permutation test*=-1.28, *P*=0.21), neither during the transition (1.07±0.26 *vs* 1.15±0.26, *paired permutation test*=-0.84, *P*=0.42) and bipedal walking (1.09±0.31 *vs* 1.07±0.25, *paired permutation test*=-0.04, *P*=0.91). There is, however, a significant difference in touch down position relative to the $BCoM$ between the contralateral legs when quadrupedal walking and the transition are compared, but not when the transition is compared to bipedal walking (Leg1-Leg2: 0.78±0.20 *vs* 1.07±0.26, *paired permutation test*=-2.80, *P*=0.002; 1.15±0.26 *vs* 1.09±0.31, *paired permutation test*=1.11, *P*=0.41, respectively; Fig. 6B.2).

When comparing consecutive footfalls of the same leg, there is a significant difference of the touch-down position relative to the $BCoM$ for both legs when quadrupedal walking and the transition are compared (Leg1: 0.72±0.20 *vs* 1.07±0.26, *paired permutation test*=-2.16, *P*=0.02; Leg2: 0.78±0.20 *vs* 1.15±0.26, *paired permutation test*=-2.87, *P*=0.0007). The transition has a significant impact on the

foot placement relative to the $BCoM$. Both legs that touch-down during the transition are positioned significantly more in front of the $BCoM$, compared to their respective position during the previous quadrupedal behaviour (Fig. 6B.2).

- *Sudden and momentary forward acceleration of the $BCoM$ plays no role in the transition*

This is already obvious from the evaluation of hypothesis 1. If there is a significant difference in the average forward speed of the subsequent sections throughout the transition, it is a decrease in speed (i.e. deceleration; see Fig. 4). Moreover, if forward acceleration would be in play, this should be reflected in the moment generated by the horizontal GRF about the $BCoM$ (see Theoretical Framework and detailed description of the worked example). Figure 7 shows the congruity index for the moment of the vertical ground reaction force and the moment of the horizontal ground reaction force with the rate of change of the total angular momentum of the body ($\dot{H}_{body}$). There is a significant difference in the congruity index of the two moments (66±10% *vs* 46±11%, *paired permutation test*=2.75, *P*=0.001). The moment of the vertical ground reaction force is more congruent with $\dot{H}_{body}$ than is the horizontal moment.

From a motor control perspective, this dynamic transition strategy, primarily involving a change in stride frequency and foot positioning, reflects adjustment of the motor coordination of the individual limb joints (Maes and Abourachid, 2013; Mori et al., 2006). Such a change in limb kinematics also affects the dynamic stability (see Fig. 3C) for reaching a new stable (bipedal) state. Hip extensor torques likely play a significant role in the initiation and control of the transition (see detailed description of the worked example). However, it does not imply any break in the coordination pattern controlled by the nervous system. The 'on the fly' quadrupedal to bipedal transition observed in baboons is therefore a good example of the shared quadrupedal and bipedal coordination in a non-adapted biped (see also Druelle et al., 2017a).

Hypothesis 3: the transition implies limited extra costs and efforts compared to the normal quadrupedal and bipedal locomotion

There is no statistical difference in the metabolic cost between the quadrupedal and bipedal walking before and after the transition (Quadrupedalism: 8.58±3.23 $J.kg^{-1}.m^{-1}$ *vs* Bipedalism: 6.45±2.78 $J.kg^{-1}.m^{-1}$; *paired permutation test*=0.72, *P'*=0.59). There is a significant difference in the metabolic cost between quadrupedal walking and the transition and between the transition and bipedal walking (Transition: 15.26±3.75 $J.kg^{-1}.m^{-1}$; *paired permutation test*=-2.29, *P'*=0.02; *Permutation test*=2.653, *P'*=0.0234, respectively; Fig. 8). On the average, the costs for the transition *sensu stricto* of a quadrupedal-bipedal 'on the fly' transition approximately doubles, compared to the costs for the preceding quadrupedal- or following bipedal walking.

These estimates of the extra costs are 'maximal' in a sense that no energy transfer or recuperation is taken into account. As already argued when discussing the worked transition example, we believe that the energetic costs to perform quadrupedal-bipedal transitions 'on the fly' are negligible when considered in the context of the normal locomotor repertoire of baboons, including gait initiations (involving abrupt accelerations), sit to stand transitions, climbing, manoeuvring, high speed gaits, etc (see further: Evolutionary perspectives).

C) Comparative aspects

To our knowledge, only one other study in primates deal with dynamic quadrupedal-bipedal transition. It was observed that *Macaca fuscata* keeps a steady forward walking speed during the quadrupedal to

bipedal transition (Nakajima et al., 2001). In addition, researchers showed that gaze was maintained (on the food reward in the context of their setup on a treadmill) by continuous changes in head orientation. Although we did not focus on gaze, we can assume that during the transition observed in baboons, the animals were targeting a point in the mirror (cf. Material and Methods). Nakajima *et al.* (2001) defined the beginning of the transition at the touch-down of the hindlimb that provokes an upward excursion of the angle of the weight bearing hip joint. This leads to free the forelimbs from the constraints of supporting the body and results in a bipedal walking gait. Although the delimitation of the transition is different from our study, the qualitative description provided by Nakajima et al. (2001) let us suggest that macaques may use a similar strategy to baboons by, at least, repositioning one hindlimb at touch-down, thus provoking the required additional positive moment about the $BCoM$. Strategies using variations in phase shift and rhythm have also been proposed, in legged robots performing a quadrupedal to bipedal transition (Aoi et al., 2012). However, as pointed out by Aoi et al. (2012) the general performance of the robots remains generally low compared to the performance observed in animals. For instance, baboons are complex organisms and use a dynamic strategy integrating stride length and frequency to make the transition 'on the fly'. A relevant observation from our study lies in the foot re-positioning relatively to the $BCoM$, the increased stride frequency and the implication of the hip extensor torques which play significant roles in the initiation and control of this transition. Some of these aspects have been implemented in the transition strategy of robots, but in a very different way than the strategy observed in baboons. Therefore, we believe that the way we describe it in this study can inspire the creation of new control strategies in robots, possibly toward more flexible abilities.

D) Evolutionary perspectives

In their daily activities, primates regularly change their posture by reorienting completely their body segments. For instance, many transitions happen in the trees (e.g. Thorpe and Crompton, 2006) which are inherent to coping with the complexity of the arboreal environment. Since decades, positional repertoires (locomotor and postural modes) are quantified by researchers to capture and frame the complexity of the locomotion of primates (e.g. Hunt et al., 1996; Prost, 1965). Although this is a relevant magnifying glass providing a good theoretical framework for many (eco-functional) purposes (Cant, 1992; Hunt, 2016), lots of these modes remain commonly irregularly performed and do not follow patterned activities (Biewener and Daley, 2007; Fleagle et al., 1981). This of course represents a challenge for further analyses and descriptions, but it also results in emerging framework including transitions between locomotor modes. Transitions must be effectively performed in many activity contexts (e.g. food carrying, display, investigation, social greetings, etc.) as well as to negotiate arboreal environments (e.g. Bailey et al., 2020; Dunham, 2015; Isler and Grüter, 2006; Myatt et al., 2011; Myatt and Thorpe, 2011; Thorpe and Crompton, 2006; Zhu et al., 2015). While body plans can be adapted to specific locomotor modes and capacities (e.g. Preuschoft, 1989; Preuschoft, 2004; Preuschoft and Günther, 1994), the capability of (arboreal) primates to transition between locomotor modes might also be under strong selective pressures.

In an evolutionary perspective, the onset of new specialised locomotor modes, such as brachiation, bipedalism, inverted quadrupedal walking, arm-swinging, etc, requires ancestors having predisposed morphologies and locomotor capabilities (Fleagle et al., 1981; Granatosky and Schmitt, 2019; Rose, 1991), in addition to the capacity to operate instantaneous locomotor transitions during their daily activities. Upright gaits obviously introduce loading constraints for the hindlimbs and increased demands in balance (Higurashi et al., 2019). However, bipedalism and quadrupedalism may share the

same basic neuromotor mechanisms, at least in non-adapted bipeds (see above; e.g. Aerts et al., 2000; Frigon, 2017; Nakajima et al., 2004; Zehr et al., 2009), which makes the relationship between these two locomotor modes even more subtle than first expected. Furthermore, bipedal walking in chimpanzees has been shown to not be significantly more costly than quadrupedalism (Kimura and Yaguramaki, 2009; Pontzer et al., 2014; Sockol et al., 2007). Our study seems to confirm this finding for locomotor costs in quadrupedal and bipedal baboons. Sockol and collaborators (2007) suggested that only few variations in morphology, such as hip extension and leg length, would have substantially improved bipedal walking efficiency above the level of quadrupedal walking efficiency in a *Pan*-like common ancestor. This hypothesis, when coupled to the results of Young et al. (2010) about the low level of interlimb integration in hominoids, and the results of Kozma et al. (2018) about hip extension in chimpanzees, let us suggest that, in early hominins, whose evolution of relatively longer legs was thus facilitated and hip extension possible, an economical bipedal walking gait was already present at this early stage of evolution (Kozma et al., 2018). As a result, considering an early hominin with increased bipedal walking capacities is possible (Kozma et al., 2018; Pontzer et al., 2014; Thompson et al., 2015; White et al., 2015). In addition, and in the light of the present results, the idea of an ancestor of hominins (in Miocene apes), capable of transitioning from one mode to another (for instance from quadrupedal to bipedal) using kinematic and dynamic strategies and avoiding significant increase in energetic inputs is possible. Early hominins and their ancestors might thus have used, amongst others, habitual bipedalism in addition to a certain form of habitual quadrupedalism, including the smooth transitions between both in their locomotor repertoire. This does not exclude, however, that other locomotor modes, like for instance suspensory locomotion or climbing, were used as well within a large locomotor repertoire as observed in extant apes.

CONCLUSION

Baboons are able to transit from quadrupedal to bipedal walking in a smooth and non-erratic way, without any significant interruption in their forward movement (i.e. making a transition on the fly). The motor strategy to do so boils down to crouching the hind parts and sprinting them underneath the rising body centre of mass. Instantaneous forward accelerations play no role. Given the short duration of the transition as such (< 1sec), the costs linked to these dynamical (on the fly) quadrupedal-bipedal transitions are estimated to be small and negligible when considered in the context of the normal locomotor repertoire of baboons. Being able, as a quadrupedal primate, to transit 'on the fly' from quadrupedal to bipedal locomotion in a smooth, rapid and apparently rather effortless way may have been important when considering the ecological/evolutionary context.

ACKNOWLEDGMENTS

We are very grateful to Guy Dubreuil, the director of the Primatology Station of the CNRS at the time the data were collected, who provided access and facilities to the animals. We are very grateful to Christophe Arnoult, the current director of the Primatology Station of the CNRS, for his support, as well as to Romain Lacoste. We thank Guillaume Daver and Zohreh Anvari for their help in recording the video sequences of quadrupedal and bipedal walking in baboons. The Technical Platform has been initially funded by the CNRS-INEE. This project is also currently funded by ANR-18-CE27-0010-01 and CNRS-INEE International Research Network IRN-GDRI0870.

CONFLICT OF INTEREST

We have no conflict of interest to declare.

AUTHORS' CONTRIBUTION

PA developed the theoretical framework, did the mechanical analysis (including code development) and wrote, together with FD, the manuscript. FD specifically dealt with the statistical analyses across the entire sample. JG was involved in a first version of the mechanical analysis. KD and GB collected the kinematical data of the walking baboons. Morphometrics of the individuals were collected by GB and FD. All authors were involved in the final discussions on the manuscript.

Data Availability

Morphometric data on the specimens are provided as supplementary material. Kinematical data will be made available on demand by the corresponding author.

Funding

Research is supported by a grant of the FWO-Flanders and the Research Council to PA (resp. K803019N and BOF/SABBAT - IDnr.: 40504). The Technical Platform has been initially funded by the CNRS-INEE. This project is also currently funded by ANR-18-CE27-0010-01 (G. Berillon Dir.), CNRS-INEE International Research Network IRN-GDRI0870.

REFERENCES

Aerts, P., Van Damme, R., D'Août, K. and Van Hooydonck, B. (2003). Bipedalism in lizards: whole-body modelling reveals a possible spandrel. *Philosophical Transactions of the Royal Society of London B: Biological Sciences* **358**, 1525-1533.

Aerts, P., Van Damme, R., Van Elsacker, L. and Duchene, V. (2000). Spatio-temporal gait characteristics of the hind-limb cycles during voluntary bipedal and quadrupedal walking in bonobos (Pan paniscus). *American Journal of Physical Anthropology* **111**, 503-517.

Alexander, R. (1997). Optimum muscle design for oscillatory movements. *Journal of Theoretical Biology* **184**, 253-259.

Alexander, R. M. (2003). Principles of animal locomotion: Princeton University Press.

Anvari, Z., Berillon, G., Asgari Khaneghah, A., Grimaud-Herve, D., Moulin, V. and Nicolas, G. (2014). Kinematics and spatiotemporal parameters of infant-carrying in olive baboons. *American Journal of Physical Anthropology* **155**, 392-404.

Aoi, S., Egi, Y., Sugimoto, R., Yamashita, T., Fujiki, S. and Tsuchiya, K. (2012). Functional roles of phase resetting in the gait transition of a biped robot from quadrupedal to bipedal locomotion. *IEEE Transactions on Robotics* **28**, 1244-1259.

Bailey, K. E., Winking, J. W., Carlson, D. L., Van Bang, T. and Long, H. T. (2020). Arm-Swinging in the Red-Shanked Douc (Pygathrix nemaeus): Implications of Body Mass. *International Journal of Primatology* **41**, 583-595.

Balter, J. E. and Zehr, E. P. (2007). Neural coupling between the arms and legs during rhythmic locomotor-like cycling movement. *Journal of neurophysiology* **97**, 1809-1818.

Berillon, G., Daver, G., D'Août, K., Nicolas, G., de la Villetanet, B., Multon, F., Digrandi, G. and Dubreuil, G. (2010). Bipedal versus Quadrupedal Hind Limb and Foot Kinematics in a Captive Sample of *Papio anubis*: Setup and Preliminary Results. *International Journal of Primatology* **31**, 159-180.

Biewener, A. A. and Daley, M. A. (2007). Unsteady locomotion: integrating muscle function with whole body dynamics and neuromuscular control. *Journal of Experimental Biology* **210**, 2949-2960.

Blickhan, R., Andrada, E., Hirasaki, E., and Ogihara, N. 2018. Global dynamics of bipedal macaques during grounded and aerial running. *Journal of Experimental Biology* **221**(24).

Blickhan, R., Andrada, E., Hirasaki, E., and Ogihara, N. 2021. Trunk and leg kinematics of grounded and aerial running in bipedal macaques. *Journal of Experimental Biology* **224**(2).

Cant, J. G. H. (1992). Positional behavior and body size of arboreal primates: A theoretical framework for field studies and an illustration of its application. *American Journal of Physical Anthropology* **88**, 273-283.

Carvalho, S., Biro, D., Cunha, E., Hockings, K., McGrew, W. C., Richmond, B. G. and Matsuzawa, T. (2012). Chimpanzee carrying behaviour and the origins of human bipedality. *Current Biology* **22**, R180-R181.

Crompton, R. H., Li, Y., Alexander, R. M., Wang, W. and Gunther, M. M. (1996). Segment inertial properties of primates: New techniques for laboratory and field studies of locomotion. *American Journal of Physical Anthropology* **99**, 547-570.

D'Août, K., Vereecke, E., Schoonaert, K., De Clercq, D., Van Elsacker, L. and Aerts, P. (2004). Locomotion in bonobos (Pan paniscus): differences and similarities between bipedal and quadrupedal terrestrial walking, and a comparison with other locomotor modes. *Journal of Anatomy* **204**, 353-361.

Demes, B. (2011). Three-dimensional kinematics of capuchin monkey bipedalism. *American Journal of Physical Anthropology* **145**, 147-155.

Dietz, V. (2002). Do human bipeds use quadrupedal coordination? *Trends in Neurosciences* **25**, 462-467.

Dietz, V., Fouad, K. and Bastiaanse, C. M. (2001). Neuronal coordination of arm and leg movements during human locomotion. *European Journal of Neuroscience* **14**, 1906-1914.

Druelle, F., Abourachid, A., Vasilopoulou-Kampitsi, M. and Aerts, P. (2022a). Convergence of bipedal locomotion: why walk or run on only two legs. In *Convergent Evolution: Animal Form and Function*, eds. V. Bels and A. P. Russel): Springer.

Druelle, F., Aerts, P. and Berillon, G. (2016). Bipedality from locomotor autonomy to adulthood in captive olive baboon (Papio anubis): Cross-sectional follow-up and first insight into the impact of body mass distribution. *American Journal of Physical Anthropology* **159**, 73-84.

Druelle, F., Aerts, P. and Berillon, G. (2017a). The origin of bipedality as the result of a developmental by-product: The case study of the olive baboon (Papio anubis). *Journal of Human Evolution* **113**, 155-161.

Druelle, F., Aerts, P., D'Août, K., Moulin, V. and Berillon, G. (2017b). Segmental morphometrics of the olive baboon (Papio anubis): a longitudinal study from birth to adulthood. *Journal of Anatomy* **230**, 805-819.

Druelle, F. and Berillon, G. (2014). Bipedalism in non-human primates: a comparative review of behavioural and experimental explorations on catarrhines. *BMSAP* **26**, 1-10.

Druelle, F., Özçelebi, J., Marchal, F. and Berillon, G. (2022b). Development of bipedal walking in olive baboons, *Papio anubis*: A kinematic analysis. *American Journal of Biological Anthropology* **177**, 719-734.

Dunham, N. T. (2015). Ontogeny of positional behavior and support use among Colobus angolensis palliatus of the Diani Forest, Kenya. *Primates* **56**, 183-192.

Fleagle, J. G., Stern, J. T., Jungers, W. L., Susman, R. L., Vangor, A. K. and Wells, J. P. (1981). Climbing: a biomechanical link with brachiation and with bipedalism. In *Symp Zool Soc Lond*, vol. 48, pp. 359-375: Symposium Zoological Society London.

Frigon, A. (2017). The neural control of interlimb coordination during mammalian locomotion. *Journal of neurophysiology* **117**, 2224-2241.

Full, R.J., and Tu, M.S. (1991). Mechanics of a rapid running insect: two-, four-and six-legged locomotion. Journal of Experimental Biology **156**(1):215-231.

Granatosky, M. C. and Schmitt, D. (2019). The mechanical origins of arm-swinging. *Journal of Human Evolution* **130**, 61-71.

Higurashi, Y., Maier, M. A., Nakajima, K., Morita, K., Fujiki, S., Aoi, S., Mori, F., Murata, A. and Inase, M. (2019). Locomotor kinematics and EMG activity during quadrupedal vs. bipedal gait in the Japanese macaque. *Journal of neurophysiology*.

Hirasaki, E., Ogihara, N., Hamada, Y., Kumakura, H. and Nakatsukasa, M. (2004). Do highly trained monkeys walk like humans? A kinematic study of bipedal locomotion in bipedally trained Japanese macaques. *Journal of Human Evolution* **46**, 739-750.

Hof, A. L. (1996). Scaling gait data to body size. *Gait & posture* **4**, 222-223.

Hunt, K. D. (1994). The evolution of human bipedality: ecology and functional morphology. *Journal of Human Evolution* **26**, 183-202.

Hunt, K. D. (2016). Why are there apes? Evidence for the co-evolution of ape and monkey ecomorphology. *Journal of Anatomy* **228**, 630-685.

Hunt, K. D., Cant, J., Gebo, D., Rose, M., Walker, S. and Youlatos, D. (1996). Standardized descriptions of primate locomotor and postural modes. *Primates* **37**, 363-387.

Isler, K. and Grüter, C. C. (2006). Arboreal locomotion in wild black-and-white snub-nosed monkeys (Rhinopithecus bieti). *Folia Primatologica* **77**, 195-211.

Kimura, T. and Yaguramaki, N. (2009). Development of Bipedal Walking in Humans and Chimpanzees : A Comparative Study. *Folia Primatologica* **80**, 45-62.

Kozma, E. E., Webb, N. M., Harcourt-Smith, W. E., Raichlen, D. A., D'Août, K., Brown, M. H., Finestone, E. M., Ross, S. R., Aerts, P. and Pontzer, H. (2018). Hip extensor mechanics and the evolution of walking and climbing capabilities in humans, apes, and fossil hominins. *Proceedings of the National Academy of Sciences*, 201715120.

Maes, L. and Abourachid, A. (2013). Gait transitions and modular organization of mammal locomotion. *Journal of Experimental Biology* **216**, 2257-2265.

Mori, S., Mori, F. and Nakajima, K. (2006). Higher nervous control of quadrupedal vs bipedal locomotion in non-human primates; Common and specific properties. In *Adaptive motion of animals and machines*, pp. 53-65: Springer.

Myatt, J., Crompton, R. and Thorpe, S. (2011). A New Method for Recording Complex Positional Behaviours and Habitat Interactions in Primates. *Folia Primatologica* **82**, 13-24.

Myatt, J. P. and Thorpe, S. K. S. (2011). Postural strategies employed by orangutans (*Pongo abelii*) during feeding in the terminal branch niche. *American Journal of Physical Anthropology* **146**, 73-82.

Nakajima, K., Mori, F., Takasu, C., Mori, M., Matsuyama, K. and Mori, S. (2004). Biomechanical constraints in hindlimb joints during the quadrupedal versus bipedal locomotion of M. fuscata. In *Progress in Brain Research*, vol. Volume 143, pp. 183-190: Elsevier.

Nakajima, K., Mori, F., Takasu, C., Tachibana, A., Okumura, T., Mori, M. and Mori, S. (2001). Integration of Upright Posture and Bipedal Locomotion in Non-Human Primates. In *Sensorimotor control*, vol. 326 eds. D. R and K. AR), pp. 95.

Nakatsukasa, M., Hirasaki, E. and Ogihara, N. (2006). Energy expenditure of bipedal walking is higher than that of quadrupedal walking in Japanese macaques. *American Journal of Physical Anthropology* **131**, 33-37.

Ogihara, N., Makishima, H., and Nakatsukasa, M. (2010). Three-dimensional musculoskeletal kinematics during bipedal locomotion in the Japanese macaque, reconstructed based on an anatomical model-matching method. *Journal of Human Evolution* **58**(3):252-261.

Pontzer, H., Raichlen, D. A. and Rodman, P. S. (2014). Bipedal and quadrupedal locomotion in chimpanzees. *Journal of Human Evolution* **66**, 64-82.

Preuschoft, H. (1989). Body shape and differences between species. *Human Evolution* **4**, 145-156.

Preuschoft, H. (2004). Mechanisms for the acquisition of habitual bipedality: are there biomechanical reasons for the acquisition of upright bipedal posture? *Journal of Anatomy* **204**, 363-384.

Preuschoft, H. and Günther, M. (1994). Biomechanics and body shape in primates compared with horses. *Zeitschrift für Morphologie und Anthropologie*, 149-165.

Prost, J. H. (1965). A Definitional System for the Classification of Primate Locomotion. *American Anthropologist* **67**, 1198-1214.

Rose, M. (1976). Bipedal behavior of olive baboons (*Papio anubis*) and its relevance to an understanding of the evolution of human bipedalism. *American Journal of Physical Anthropology* **44**, 247-261.

Rose, M. (1991). The process of bipedalization in hominids. In *Origine(s) de la bipédie chez les hominidés*, eds. C. Y and S. B), pp. 37-48. Paris: Editions du Centre National de la Recherche Scientifique.

Rosen, K. H., Jones, C. E. and DeSilva, J. M. (2022). Bipedal locomotion in zoo apes: Revisiting the hylobatian model for bipedal origins. *Evolutionary Human Sciences* **4**.

Sockol, M. D., Raichlen, D. A. and Pontzer, H. (2007). Chimpanzee locomotor energetics and the origin of human bipedalism. *Proceedings of the National Academy of Sciences* **104**, 12265-12269.

Stanford, C. B. (2006). Arboreal bipedalism in wild chimpanzees: Implications for the evolution of hominid posture and locomotion. *American Journal of Physical Anthropology* **129**, 225-231.

Thompson, N. E., Demes, B., O'Neill, M. C., Holowka, N. B. and Larson, S. G. (2015). Surprising trunk rotational capabilities in chimpanzees and implications for bipedal walking proficiency in early hominins. *Nature communications* **6**.

Thompson, N. E., Rubinstein, D., Parrella-O'Donnell, W., Brett, M. A., Demes, B., Larson, S. G. and O'Neill, M. C. (2021). The loss of the 'pelvic step' in human evolution. *Journal of Experimental Biology* **224**, jeb240440.

Thorpe, S. K. S. and Crompton, R. H. (2006). Orangutan positional behavior and the nature of arboreal locomotion in Hominoidea. *American Journal of Physical Anthropology* **131**, 384-401.

Videan, E. N. and McGrew, W. C. (2001). Are bonobos (Pan paniscus) really more bipedal than chimpanzees (*Pan troglodytes*)? *American Journal of Primatology* **54**, 233-239.

Videan, E. N. and McGrew, W. C. (2002). Bipedality in chimpanzee (*Pan troglodytes*) and bonobo (*Pan paniscus*): Testing hypotheses on the evolution of bipedalism. *American Journal of Physical Anthropology* **118**, 184-190.

White, T. D., Lovejoy, C. O., Asfaw, B., Carlson, J. P. and Suwa, G. (2015). Neither chimpanzee nor human, Ardipithecus reveals the surprising ancestry of both. *Proceedings of the National Academy of Sciences* **112**, 4877-4884.

Wrangham, R. W. (1980). Bipedal locomotion as a feeding adaptation in gelada baboons, and its implications for hominid evolution. *Journal of Human Evolution* **9**, 329-331.

Young, N. M., Wagner, G. P. and Hallgrimsson, B. (2010). Development and the evolvability of human limbs. *Proceedings of the National Academy of Sciences* **107**, 3400-3405.

Zehr, E. P., Hundza, S. R. and Vasudevan, E. V. (2009). The quadrupedal nature of human bipedal locomotion. *Exercise and sport sciences reviews* **37**, 102-108.

Zhu, W.-W., Garber, P. A., Bezanson, M., Qi, X.-G. and Li, B.-G. (2015). Age-□and sex-based patterns of positional behavior and substrate utilization in the golden snub-nosed monkey (Rhinopithecus roxellana). *American Journal of Primatology* **77**, 98-108.

Figures

A

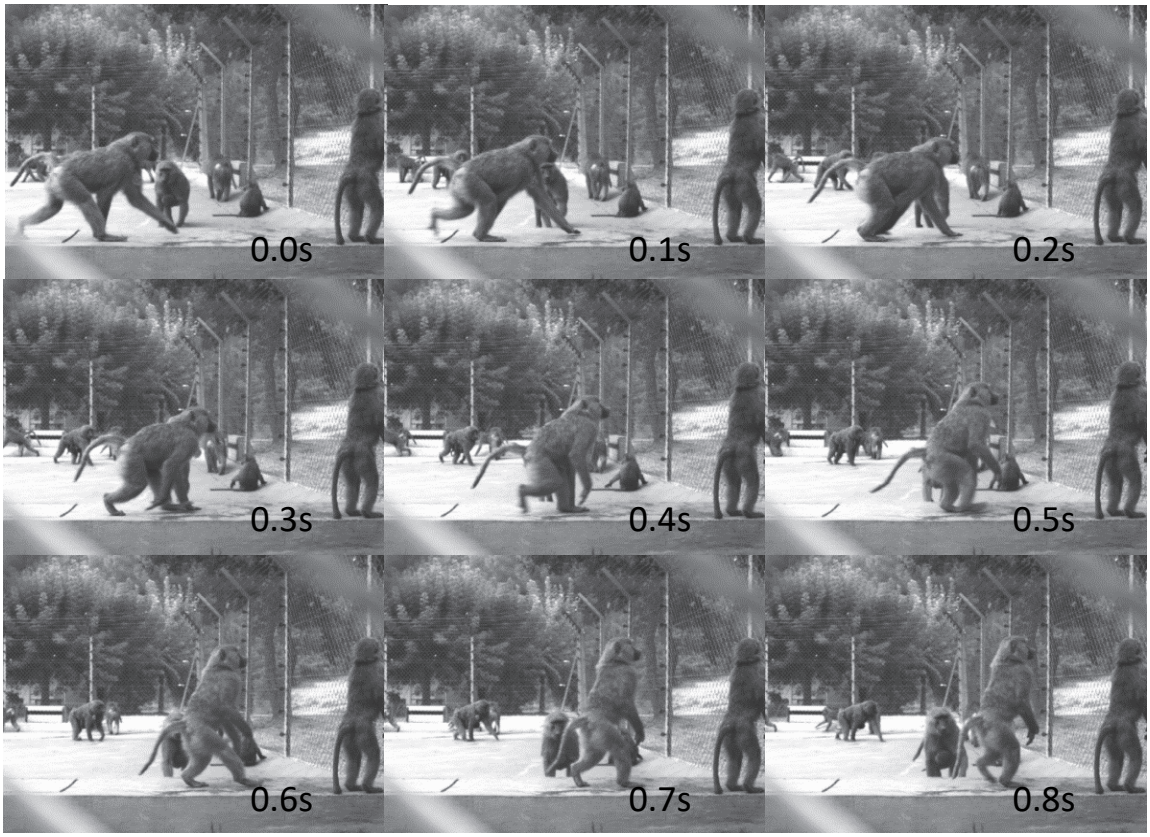

B

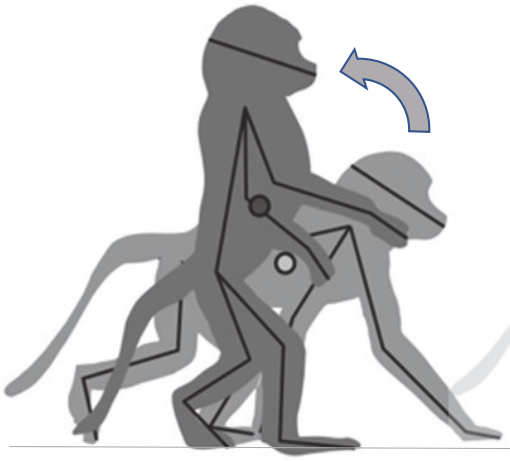

C

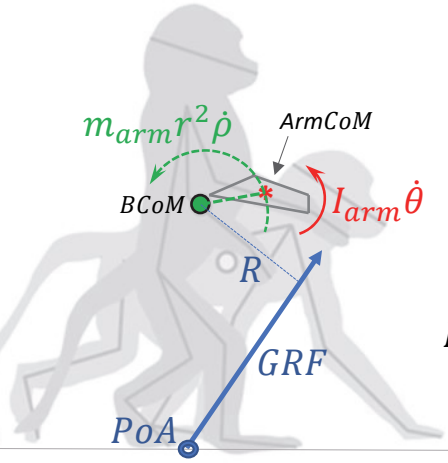

$$H_{arm} = I_{arm}\dot{\theta} + m_{arm}r^2\dot{\rho}$$

$$H_{body} = \sum_{i=1}^{n} H_{segment_{(i)}}$$

$$\dot{H}_{body} = M_{GRF} = R \times GRF$$

Figure 1. A) Representative illustration of a quadrupedal-bipedal transition 'on the fly' in a walking sequence of a baboon**.** B): outlines of start and end posture of a quadrupedal-bipedal transition 'on the fly'. C) The angular momentum of the total body (H_{body}) is the sum of the angular momenta of all segments; each segmental angular momentum (for instance, H_{arm} for the lower arm) equals the sum of its local ($I_{arm}\dot{\theta}$) and its remote ($m_{arm}r^2\dot{\rho}$) term; $\dot{H}_{body}$ (instantaneous change of H_{body}) equals the moment of the ground reaction force ($R \times GRF$ =M_{GRF}) [with I_{arm}= moment of inertia of the arm about its Centre of Mass (CoM; red asterisk), $\dot{\theta}$ = instantaneous angular velocity of the arm about its CoM, m_{arm}= arm mass, *r* = instantaneous distance from *ArmCoM* to $B(ody)Com$, $\dot{\rho}$ = instantaneous angular velocity of *ArmCoM* about $BCoM$, GRF = Ground Reaction Force, R = moment arm GRF about $BCoM$, PoA = point of application GRF*].*

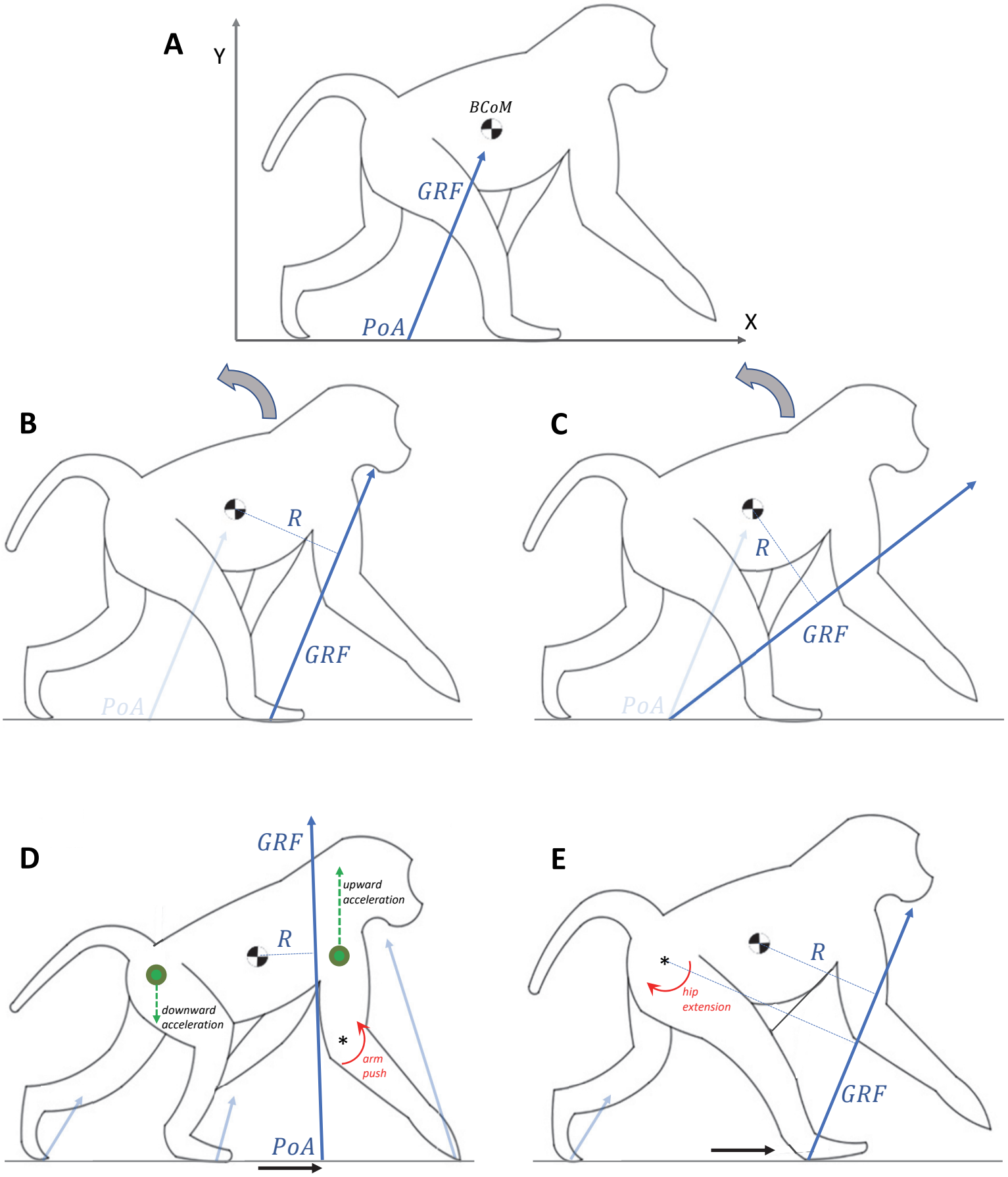
A
Y
X
BCoM
GRF
PoA
B
R
GRF
PoA
C
R
GRF
PoA
D
GRF
upward
acceleration
R
downward
acceleration
*
arm
push
PoA
E
*
hip
extension
R
GRF

Figure 2. Imaginary 'stills' from a walking sequence of a quadruped (abbreviations as in Fig. 1). According conditions applying at the instant shown in (A), GRF has no moment about the $BCoM$, (hence $\dot{H}_{body}$=0). To generate a counterclockwise moment (hence $\dot{H}_{body}$>0), the PoA can be shifted forward (B) and/or GRF can be oriented more horizontally (C). Larger moments can further be realised by increasing the amplitude of GRF (C). Similar, but opposite shifts and reorientations result in a clockwise moment (hence $\dot{H}_{body}$ <0). Options to generate a counterclockwise moment about the $BCoM$ during the early quadrupedal bipedal transition 'on the fly' (D) when still on all four and (E) when fore limbs have lost contact with the ground. (Abbreviations as in Fig. 1; see text for more explanation; *: joint rotation centres).

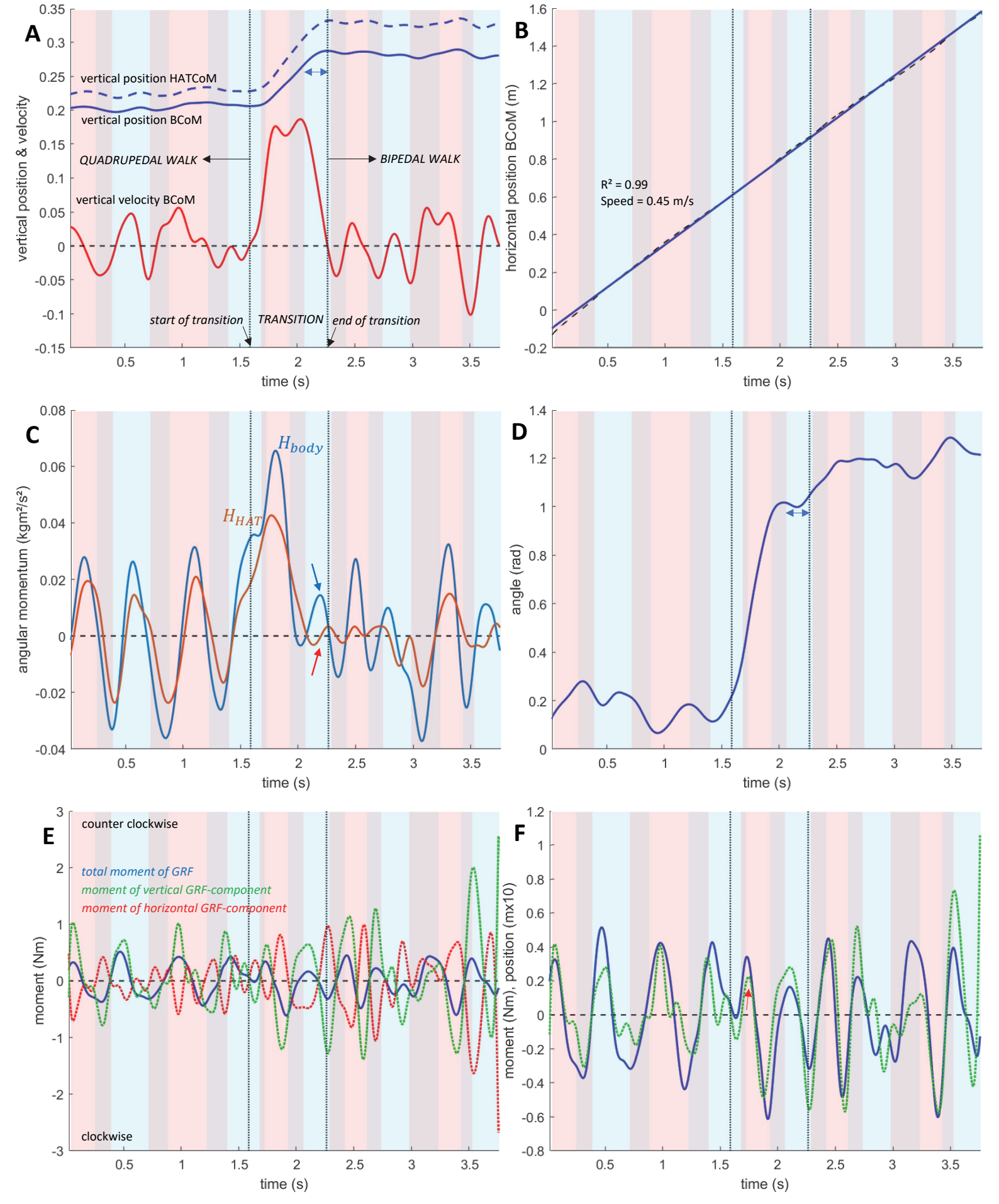
A
vertical position & velocity
vertical position HATCoM
vertical position BCoM
QUADRUPEDAL WALK
BIPEDAL WALK
vertical velocity BCoM
start of transition
TRANSITION
end of transition
time (s)
B
horizontal position BCoM (m)
R² = 0.99
Speed = 0.45 m/s
time (s)
C
angular momentum (kgm²/s²)
H_{body}
H_{HAT}
time (s)
D
angle (rad)
time (s)
E
counter clockwise
total moment of GRF
moment of vertical GRF-component
moment of horizontal GRF-component
clockwise
moment (Nm)
time (s)
F
moment (Nm), position (mx10)
time (s)

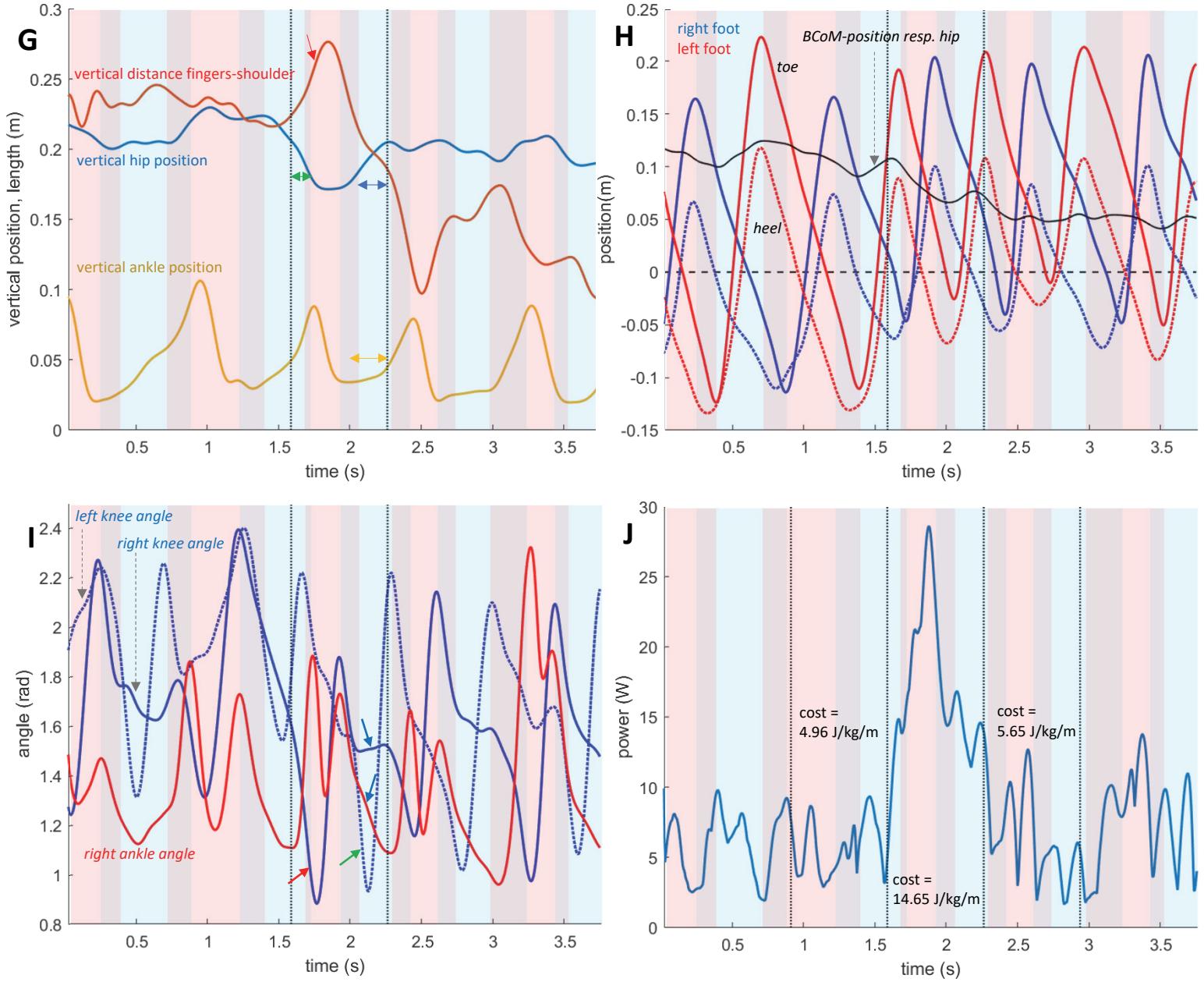
G
vertical distance fingers-shoulder
vertical hip position
vertical ankle position
vertical position, length (m)
time (s)
H
right foot
left foot
toe
heel
BCoM-position resp. hip
position(m)
time (s)
I
left knee angle
right knee angle
right ankle angle
angle (rad)
time (s)
J
cost =
4.96 J/kg/m
cost =
14.65 J/kg/m
cost =
5.65 J/kg/m
power (W)
time (s)

Figure 3. Analysis of quadrupedal-bipedal transition 'on the fly' (worked example; see text). All panels: vertical dashed black lines indicate the start and end of the transition phase; blue and red shaded zones indicate the stance phases of the right (camera-side) and left (contralateral side) foot, respectively. A: determination of the transition period. The vertical velocity profile of the $BCoM$ (red) bounds the transition phase (zero-crossing). The double headed arrow refers to the period the $BCoM/HATCoM$ still rise despites the angular momenta (panel C) are close to zero (for details, see text); B: forward displacement of the $BCoM$ (dashed black) and its linear regression (blue; for details, see text); C: total angular moment of the body and HAT. The red arrow indicates that the H_{HAT} is close to zero in the time-period spanned by the double arrow in panel A. The blue arrow thus shows that, in this time span, the total body momentum is entirely captured in the moving hind limbs (for details, see text); D: angular position of the trunk. The double arrow spans the same period as in panel A, during which no trunk rotation happens (linked to panel G;for details, see text); E: moment of the total (blue), vertical (dashed green) and horizontal (dashed red) GRF about the $BCoM$. From the timing and direction of the oscillations, it is obvious that the total moment (blue; equal to the rate of change of the total angular momentum in panel C) is entirely determined by the vertical GRF -component (green; for details, see text); F: moment of the total GRF (blue) and PoA with respect of the $BCoM$ (dashed green). Again, timing and direction of the oscillations coincide indicating that the (rate of) change of the total angular momentum is primarily determined by PoA -shifts (for details, see text); G: vertical hip (blue) and ankle (ocher) displacement and vertical distance between shoulder and fingers tips (red). The double headed blue arrow is as in panels D and A. During this time span, the hip moves up thus standing for the rise of the $BCoM$ and HATCoM (panel A). The time periode spanned by the double headed green arrow coincides with downwards acceleration of the hip (hind parts) and can thus stand for an early forwards shift of the PoA (arrow in panel F). The red arrow points at the instant the front limbs no longer contact the ground (no further potential contribution by arm pushing). The time period spanned by the double headed ocher arrow indicate the height gain of the ankle as a result of tarso-metatarsal dorsi flexion. Since the knee is hardly extending during this time span (blue arrow in panel I), this mechanism assist the above mentioned hip rise (for details, see text); H: relative fore-aft positioning of the feet and the $BCoM$ with respect to the hip's (horizontal) position. Toe/heel are contacting the ground whenever the according profile moves backwards with respect to the hip (i.e. decreasing relative position). In this way, stance periods are determined. The $BCoM$ (black) moves backward with respect to the hip during most of the transition phase (except for the period spanned by the blue double headed arrow in panels D and A) as a result of the upwards HAT (trunk) rotation. (for details, see text); I: knee (blue) and ankle (red) angles. The red arrow indicates the continued deep stance knee flexion when transition initiates. A similar deep knee flexion is present during the next contralateral stance (green arrow). During the subsequent stance of the limb that initiates transition, the knee angle remains nearly constant (blue arrow at knee profile), whereas the ankle joint of the same limb decreases (blue arrow at ankle profile). This implies the forward rotation of the fixed hip-knee-ankle-triangle about. (for details, see text); J: instantaneous metabolic power (conservative estimate: no transfer or elastic recovery) and metabolic costs for the transition period and a quadrupedal and bipedal period of identical duration as indicated by the additional vertical black dashed lines (for details, see text).

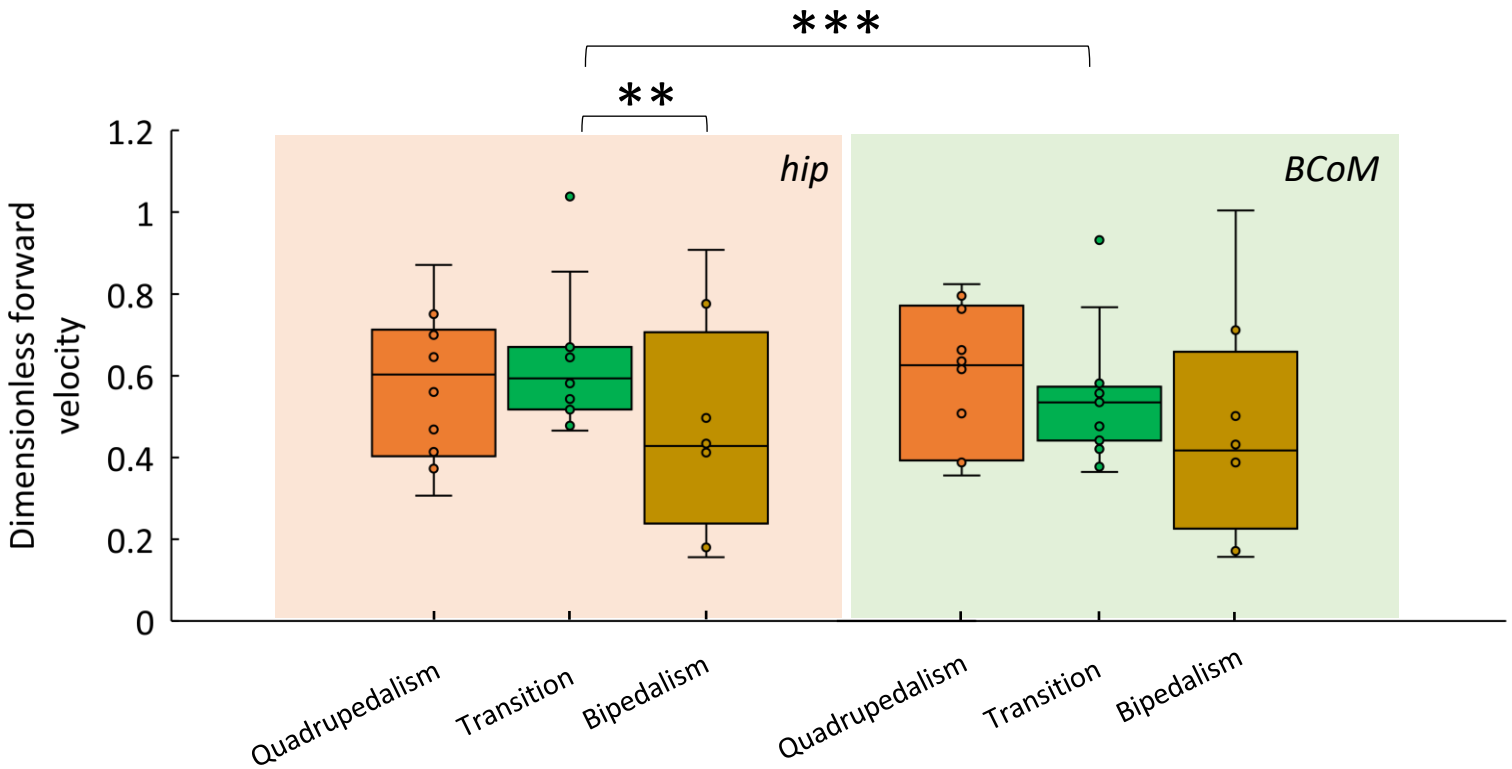
***
**
hip
BCoM
Dimensionless forward velocity
1.2
1
0.8
0.6
0.4
0.2
0
Quadrupedalism
Transition
Bipedalism
Quadrupedalism
Transition
Bipedalism

Figure 4. Box plots of the dimensionless forward velocity throughout the transition, estimated from the hip joint and from the $BCoM$. Box shows 25th and 75th percentiles with median. Symbol significance: **P<0.01, ***P<0.0001.

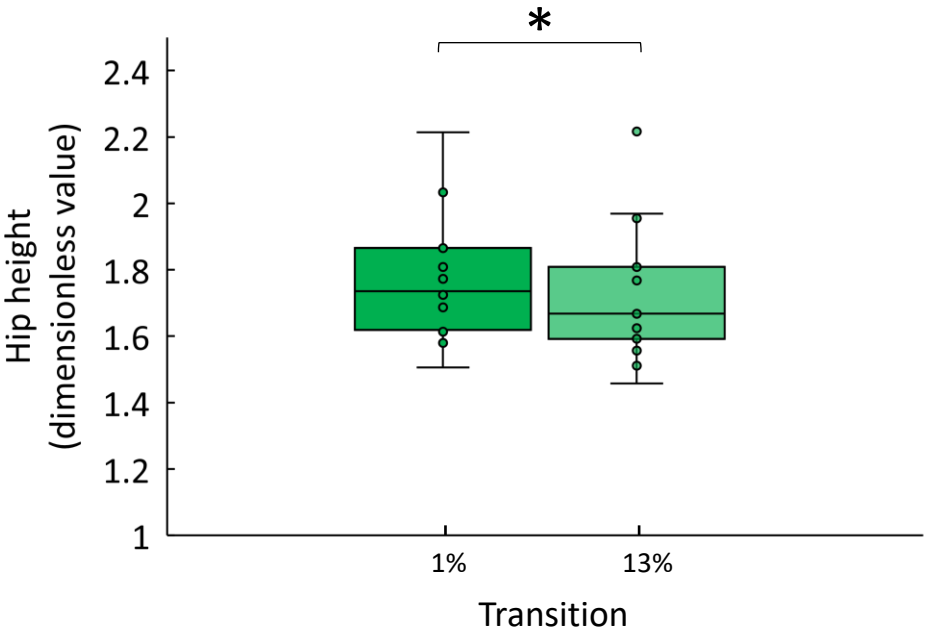
*
2.4
2.2
2
1.8
1.6
1.4
1.2
1
Hip height
(dimensionless value)
1%
13%
Transition

Figure 5. Box plots of the dimensionless hip height at the start of the transition and at 13% of the transition period. Box shows 25^{th} and 75^{th} percentiles with median. Symbol significance: *P<0.05.

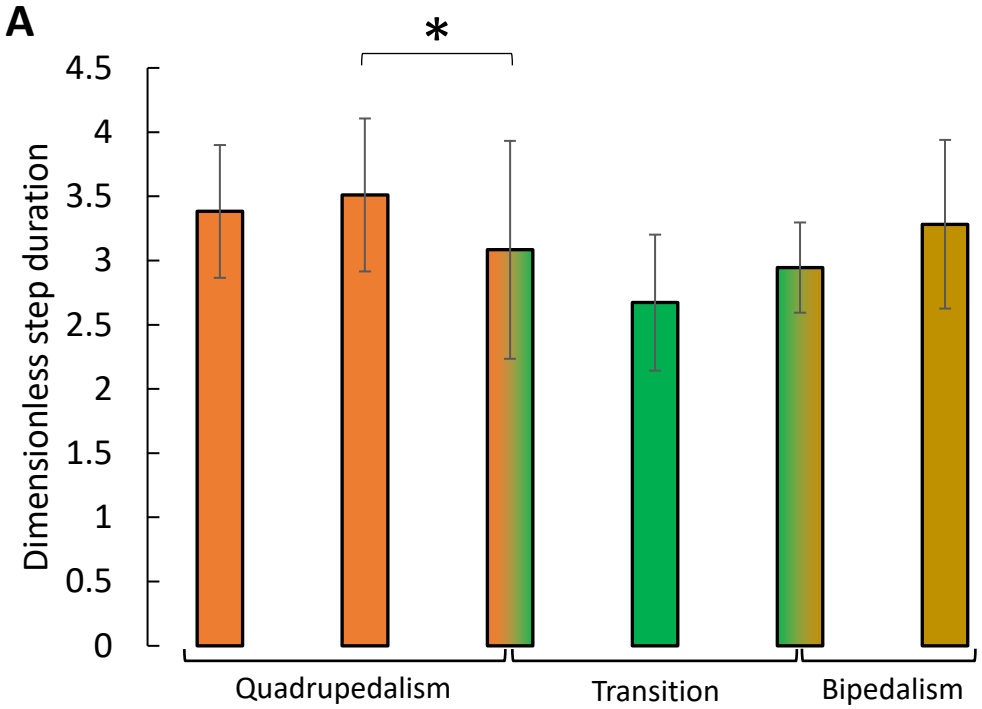
A
*
4.5
4
3.5
3
2.5
2
1.5
1
0.5
0
Dimensionless step duration
Quadrupedalism
Transition
Bipedalism

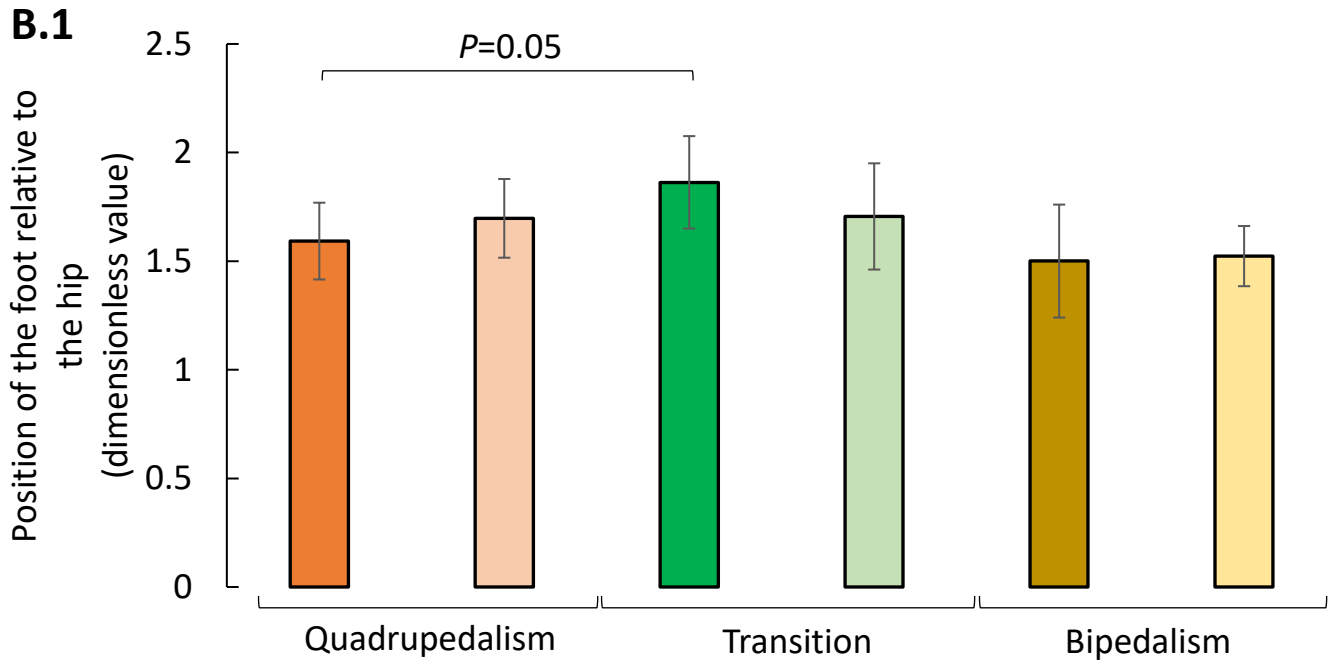
B.1
P=0.05
2.5
2
1.5
1
0.5
0
Position of the foot relative to the hip (dimensionless value)
Quadrupedalism
Transition
Bipedalism

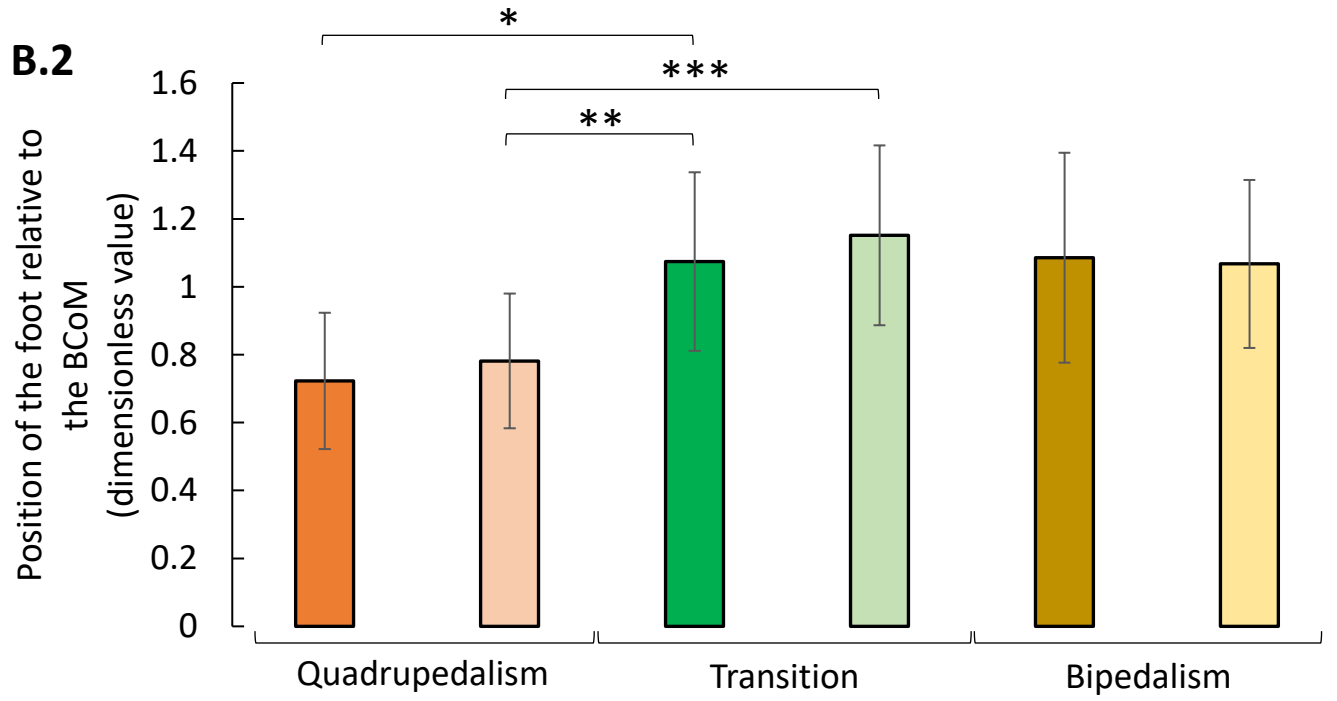
B.2
*
***
**
1.6
1.4
1.2
1
0.8
0.6
0.4
0.2
0
Position of the foot relative to the BCoM (dimensionless value)
Quadrupedalism
Transition
Bipedalism

Figure 6. A: Dimensionless step duration of the hindlimbs throughout the quadrupedal to bipedal transition (orange: quadrupedal, green: transition; ochre: bipedal). B.1: Touch-down positions of the foot relative to the hip and B.2 to the $BCoM$ after size correction (orange: quadrupedal; green: transition; ochre: bipedal; dark-coloured: leg1; light-coloured: leg2). Symbol significance: *P<0.05, **P<0.01, ***P<0.0001.

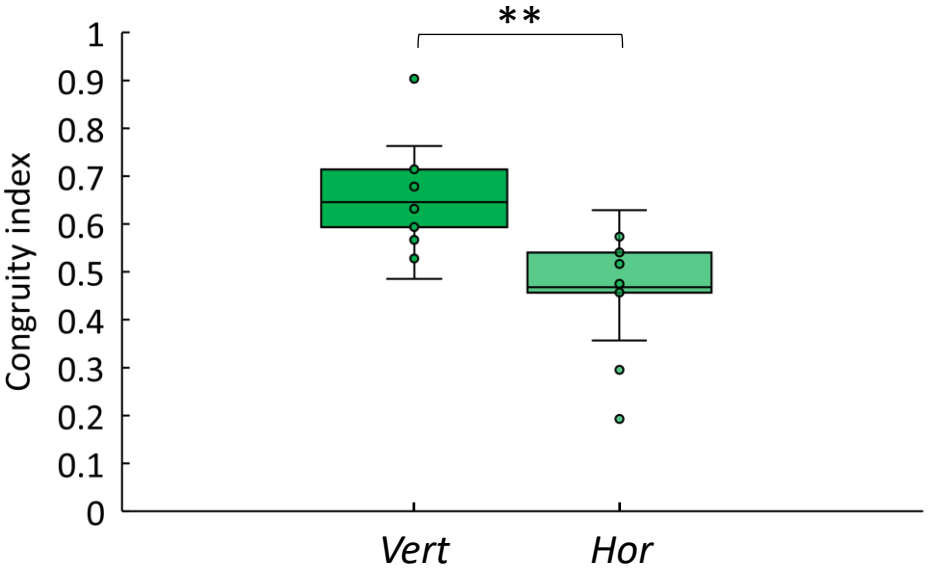
**
Congruity index
1
0.9
0.8
0.7
0.6
0.5
0.4
0.3
0.2
0.1
0
Vert
Hor

Figure 7. Box plots of the congruity indices of the moments of the planar components of the GRF with the total angular momentum of the body ($\dot{H}_{body}$) during the transition. Box shows 25th and 75th percentiles with median. Symbol significance: $^{**}P<0.01$.

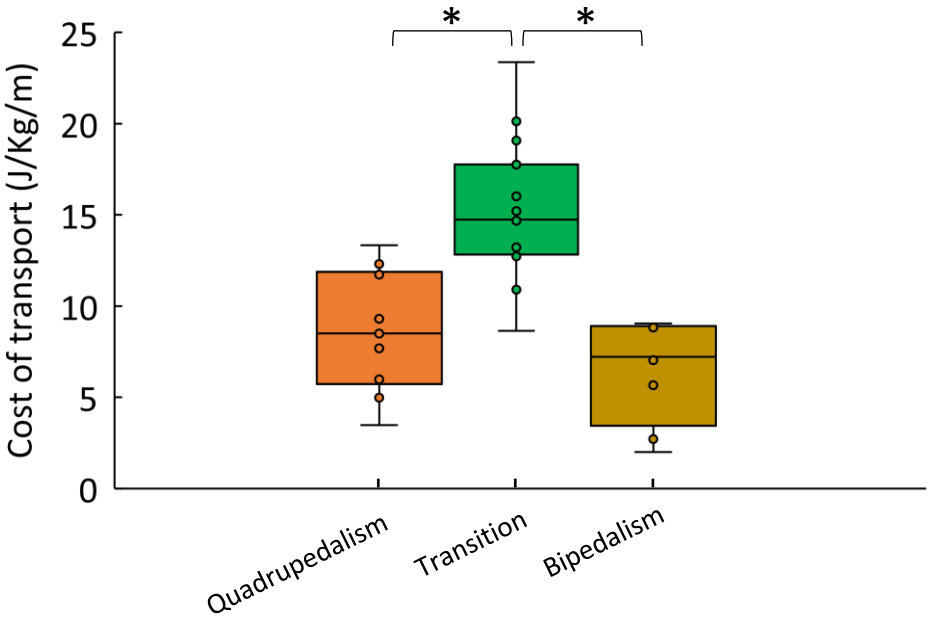
Cost of transport (J/Kg/m)
25
20
15
10
5
0
*
*
Quadrupedalism
Transition
Bipedalism

Figure 8. Box plots of the cost of transport throughout the transition. Box shows 25th and 75th percentiles with median. Symbol significance: *P<0.05.

Supplementary Material

1) S1- Morphometrics of the specimens

TABLE A. Individual morphometrics

ID	V916F	V936G	V902G	V792BA	V896BB	V792BB	V936H	V936G	V908GA	V908I
Name	Babar	Fleur	Céline	Chris	Dédé	Dictée	Emeraude	Carbone[2]	Epine	Chantal[3]
Mass	16.12	2.85	7.62	10.33	7.26	6.37	5.45	3.59	5.86	14.08
Age[1]	4.75	0.93	3.76	3.60	2.70	2.16	1.96	1.17	2.12	5.65
Sex	M	F	F	M	M	F	F	F	F	F
Length (mm)										
Hand	135	85	110	120	105	105	95	95	98	125
Forearm	205	125	172	180	166	152	148	131	155	198
Arm	192	115	152	175	158	145	135	120	145	185
Thigh	200	120	170	182	158	145	138	130	145	194
shank	203	123	170	185	160	148	148	125	150	197
Foot	195	125	160	178	147	148	148	129	149	179
Trunk	422	235	343	389	315	338	275	270	310	425
Head	188	118	150	164	147	142	138	124	140	175
Tail	447	282	320	360	360	348	346	295	350	448
Mass (kg)										
Hand	0.16	0.04	0.08	0.11	0.08	0.07	0.06	0.05	0.06	0.13
Forearm	0.32	0.07	0.17	0.19	0.15	0.16	0.11	0.08	0.14	0.25
Arm	0.55	0.06	0.21	0.32	0.25	0.19	0.15	0.09	0.17	0.45
Thigh	1.26	0.15	0.56	0.84	0.51	0.46	0.34	0.21	0.39	1.35
Shank	0.38	0.07	0.16	0.26	0.16	0.13	0.13	0.08	0.13	0.40
Foot	0.30	0.06	0.14	0.17	0.13	0.12	0.11	0.08	0.10	0.26
Trunk	7.42	1.19	3.45	4.88	2.97	2.87	2.29	1.58	2.92	7.33
Head	1.73	0.40	0.80	1.09	0.84	0.75	0.60	0.48	0.63	1.29
Tail	0.29	0.06	0.12	0.18	0.17	0.14	0.11	0.07	0.11	0.34
CoM position relative to the proximal joint										
Hand	0.41	0.42	0.40	0.41	0.43	0.43	0.42	0.40	0.44	0.41
Forearm	0.44	0.42	0.43	0.42	0.43	0.42	0.41	0.43	0.42	0.43
Arm	0.44	0.49	0.45	0.45	0.45	0.45	0.45	0.46	0.45	0.42
Thigh	0.40	0.43	0.40	0.40	0.38	0.38	0.41	0.38	0.39	0.41
Shank	0.47	0.45	0.46	0.46	0.47	0.48	0.47	0.48	0.47	0.45
Foot	0.32	0.37	0.37	0.34	0.36	0.34	0.36	0.34	0.36	0.37
Trunk	0.51	0.52	0.51	0.52	0.52	0.53	0.52	0.53	0.53	0.51
Head	0.43	0.46	0.44	0.43	0.45	0.45	0.45	0.44	0.45	0.44
Tail	0.32	0.32	0.32	0.32	0.32	0.32	0.32	0.32	0.32	0.32
Moment of inertia about the proximal joint (kg.mm²)										
Hand	717.68	66.00	218.41	377.40	242.93	198.93	133.80	98.51	167.01	481.58
Forearm	3648.82	288.41	1361.01	1581.04	1117.20	891.73	590.89	357.83	856.64	2587.26
Arm	5498.16	272.12	1344.35	2734.00	1738.06	1127.21	767.64	360.57	995.80	3933.80
Thigh	11921.47	584.22	3846.64	6525.52	2879.59	2179.98	1618.70	791.05	1879.80	12591.87
Shank	4714.34	303.35	1326.53	2536.59	1271.93	890.56	858.44	385.88	893.51	4355.05
Foot	1903.07	181.83	749.80	989.69	530.30	498.80	449.51	236.98	436.77	1708.44
Trunk	446341.26	23173.62	138764.27	257183.75	103030.05	116893.55	60778.67	40756.22	99455.28	451971.18

Head	16173.36	1598.55	4868.12	7774.25	5015.79	4212.21	3140.18	2004.22	3384.26	10838.66
Tail	9082.20	714.91	1844.82	3742.82	3348.28	2634.30	2134.73	914.63	2160.09	10668.16
Moment of inertia about the CoM (kg.mm²)										
Hand	225.21	20.06	70.26	118.43	71.31	57.20	40.61	31.53	47.41	152.36
Forearm	1054.21	87.92	389.99	488.91	326.67	265.01	187.09	107.28	254.85	773.11
Arm	1587.88	74.83	381.55	790.36	488.81	318.79	221.39	100.33	289.54	1206.94
Thigh	3858.67	176.77	1209.62	2129.65	993.89	759.66	512.99	281.08	636.20	3976.26
Shank	1210.42	84.49	358.01	694.31	337.35	245.66	225.91	106.75	234.99	1166.87
Foot	746.46	61.62	252.79	359.31	187.45	182.58	156.24	86.79	150.61	576.30
Trunk	104952.39	5145.15	31151.43	57747.66	23704.74	26064.80	13876.37	8893.06	22079.91	105842.60
Head	4704.58	420.21	1375.83	2268.19	1396.83	1181.92	856.97	559.40	927.80	3004.27
Tail	3132.73	246.40	636.54	1292.10	1155.32	908.71	735.90	315.25	744.54	3682.07

[1]Note that the age of the individuals slightly varies from Table 1 as the individuals were not measured the same day as the recording day of the quadrupedal-bipedal transition sequence.
[2]Carbone replaces Filosophie
[3]Chantal replaces Ursuline

2) S2- MP4: Animated stick-figure of the quadrupedal-bipedal transition of the worked example. The individual (Fleur, 2.85 kg, hip height in bipedal posture = ~0.2 m) walks at a speed of 0.45 m/s (see manuscript for more details). The (relative magnitude, orientation and position of the GRF regarding the $BCoM$ are shown.
3) S3- MP4: Animated stick-figure of the quadrupedal-bipedal transitions of Babar (16.12 kg; upper level of the size range of the of the baboon group, 0.75 m/s), Dede (7.26 kg; middle of the size range of the of the baboon group, 0.40 m/s) and Filosophie (3.59kg; lower level of the size range of the of the baboon group, 0.56 m/s). For data on individuals see table 1 of supplementary material S1).